

WAVE HEIGHTS AND SET-UP
IN A SURF ZONE

By I. A. Svendsen

Dept. of Civil Engineering
University of Delaware^{*)}

April 1983

^{*)} On leave from Inst. of Hydrodyn. and Hydraul. Engrg.,
Technical University of Denmark.

ABSTRACT

A theoretical model is developed for wave heights and set-up in a surf zone. In the time averaged equations of energy and momentum the energy flux, radiation stress and energy dissipation are determined by simple approximations which include the surface roller in the breaker. Comparison with measurements shows good agreement. Also the transitions immediately after breaking are analysed and shown to be in accordance with the above mentioned ideas and results.

1. INTRODUCTION

The proper modeling of wave motion in the surf zone on a littoral coast has been the goal of many investigations in particular in the last two decades. Yet in spite of progress both in terms of a growing stock of reliable experimental results and in theoretical understanding of the processes the general impression of the situation today is still that much remains to be done.

The present investigation is mainly theoretical but relies heavily on experimental evidence at a number of points. It also indirectly leans on the many contributions in the literature which have helped to show that conventional wave theories cannot be used to describe surf zone waves.

As in most of those contributions we only consider integral properties of the waves and work with equations time averaged over a wave period. The goal is only to describe the wave height and mean water level (set-up) variations. This means that the integral wave properties we need to determine first of all are energy flux, radiation stress and energy dissipation.

In spite of the fact that integral properties should be less sensitive to minor inaccuracies in the details of the wave description it is generally accepted that linear wave theory is too different to yield a proper description of energy flux and radiation stress in the surf zone. Some authors have tried to use solitary wave theory (see e.g., Divoky et al., 1968), cnoidal theory or hyperbolic wave theory (James, 1974, is an example) which are other easily accessible wave theories. For reasons that

may become clear from the present contribution these particular suggestions do not work, but this conclusion is often concealed by the fact that results obtained for the wave heights and set-up also depend on how the energy dissipation is modelled.

Also the idea of a similarity solution for the waves has been pursued. Such an approach is more likely to be able to lead to acceptable results, although in the form presented by Wang & Yang (1980) it implicitly assumes that the wave height to water depth is a constant which we know is not the case (see e.g., the experimental results by Horikawa & Kuo (1966), and also this paper).

In acknowledgement of the limited success of the theoretical investigations and the access to modern measuring techniques such as LDA, contributions have been published giving both very detailed measurements of velocity and pressure fields and computations of particularly radiation stress and momentum balance from the basic definitions (see Stive, 1980, and Stive & Wind, 1982).

The possibilities for evaluating the energy dissipation are far more restricted. In principle turbulence is created by two sources: the bottom boundary layer and the surface breaker. In practice, however, the bottom dissipation is totally outweighed by the dissipation due to breaking, and is consequently neglected here.

The idea which turns out to be most fruitful in determining the energy dissipation (if a detailed description of the turbulent flow is not attempted) is based on the resemblance of surf zone waves with bores. This

5

was discussed by LeMehauté (1962) and later by Divoky et al. (1968). To fit measurements, however, they used the motion of a non-saturated breaker suggested by LeMehauté (1962), which implies an energy dissipation smaller than the dissipation in a hydraulic jump of the same height as the wave. This is the opposite result of that found by Svendsen et al. (1978) who concluded that the dissipation in actual measurements were larger than in a jump of the same height. The explanation for this controversy probably lies in the different values used for the energy flux. In section 7 we will see that in a cnoidal or solitary wave (used for assessing the energy flux by Divoky et al.) the energy flux for a given wave height is much smaller than in a surf zone wave. Hence the smaller dissipation required by Divoky et al. for a given (measured) wave height decrease.

In the present paper we simply use the hydraulic jump expression for the energy dissipation. This is in realization of two facts.

Firstly Svendsen & Madsen (1981) essentially confirmed the conclusion in Svendsen et al. (1978) (in the following denoted I), but their results indicate that many factors are involved, and further studies show that the deviation from the hydraulic jump dissipation in most cases is less than 20%.

Secondly the other effects studied in the following are found to be more important.

The paper may be considered a continuation of the work reported in I. To determine the wave height and set-up variation we consider the equations of energy and momentum balance, both averaged over the wave period (section 2), and in section 3 derive a closed form solution to the energy equation. In

section 4 we investigate an analytical solution for a special case. This reveals that neglecting set-up there is only one parameter K (given by the wave properties at the starting point) which determines the wave heights. K is a combination of the bottom slope parameter $S = h_x L/h$ identified for shoaling by Svendsen & Hansen (1976) (h_x is bottom slope, L wave length and h water depth), the wave height to water depth ratio H/h and the dimensionless energy flux B .

The three wave properties mentioned earlier (the energy flux, radiation stress and energy dissipation) are determined in section 5. Here it becomes necessary to concentrate on the inner region (defined in I) of the surf zone where the waves have become bore-like (Fig. 1). It is shown that the most important feature is the existence of a surface roller which to the first approximation can be considered as a volume of water carried with the wave. The roller almost doubles both energy flux and radiation stress relative to a shallow water wave otherwise of the same shape.

Fig. 1

Section 6 shows comparison with experimental results in the inner region. Both wave heights and set-up are well predicted.

When it comes to the outer region (Fig. 1), however, some paradoxical features are identified in the measurements (section 7). The paradox is resolved by considering jump conditions analogous to those applied for bores and hydraulic jumps. This implies using the momentum and energy equations for the entire outer region. The results show that the expressions derived

in Section 5 for waves in the inner region are consistent with results for waves before breaking.

Throughout the derivations the simplest and lowest order approximations have been used. Thus many details such as non-uniform velocity profiles, the effect of the strong turbulence, etc. are simply neglected. The reason is that these aspects, however important, turn out to be minor corrections relative to the effects included. Hence the following is meant as an attempt to show that it is possible for the wave motion in a surf zone to formulate a crude model which reproduces all the major features observed in the measurements.

2. THE BASIC EQUATIONS

We consider the two dimensional problem sketched in Fig. 2 which also shows the definition of variables.

Fig. 2

The three basic equations to be satisfied represent the conservation of mass, momentum and energy, integrated over depth and averaged over a wave period T .

The conservation of mass will not be invoked explicitly but used in the way the particle velocities in the wave are evaluated.

We consider regular progressive waves only and hence the momentum equation simply reads

$$\frac{\partial S_{xx}}{\partial x} = - \rho g (h + \bar{\eta}) \frac{\partial \bar{\eta}}{\partial x} \quad (2.1)$$

where S_{xx} is the radiation stress defined (exactly) by ($\bar{\quad}$ denoting average over a wave period)

$$\left. \begin{aligned} S_{xx} &= F_m + F_p \\ F_m &= \overline{\int_{-h}^{\eta} \rho u^2 dz} \quad ; \quad F_p = \overline{\int_{-h}^{\eta} p_D dz} - \frac{1}{2} \rho g \bar{\eta}^2 \end{aligned} \right\} \quad (2.2)$$

with the dynamic pressure p_D given by

$$p_D = \rho g z + p \quad (2.3)$$

Using E_f for mean energy flux and \mathcal{D} for energy dissipation, the energy equation (also averaged over a wave period) becomes

$$\frac{\partial E_f}{\partial x} = \mathcal{D} \quad (2.4)$$

The general definition of E_f is

$$E_f = \overline{\int_{-h}^{\eta} [p_D + \frac{1}{2} \rho (u^2 + v^2 + w^2)] u \, dz} \quad (2.5)$$

In both (2.3) and (2.5) velocities and pressures are the instantaneous values, so that these definitions also cover the turbulent flow situations in a surf zone. Since, however, any ordered mechanical energy that is turned into turbulence will be reduced to heat within roughly the following wave period we shall choose in (2.4) to consider only the flux of (ordered) wave energy, that is, consider energy lost as soon as it has been changed to turbulence. To illustrate this we write

$$E_f = E_{f,w} + E'_f \quad (2.6)$$

where E'_f is the total flux of turbulent energy (by all means, including diffusion) and (with $\tilde{v} = 0$)

$$E_{f,w} = \overline{\int_{-h}^{\eta} (\tilde{p}_D + \frac{1}{2} \rho (\tilde{u}^2 + \tilde{w}^2)) \tilde{u} \, dz} \quad (2.7)$$

($\tilde{}$ denoting ensemble averaged values) is the flux of "wave energy."

Hence (2.4) becomes

$$\frac{\partial E_{f,w}}{\partial x} = \mathcal{D} - \frac{\partial E'_f}{\partial x} = \mathcal{D}_t \quad (2.8)$$

where \mathcal{D}_t then equals minus the production of turbulent energy.

But in the steady wave motion considered \mathcal{D}_t also equals minus the energy dissipation \mathcal{D} .

Hence in (2.4) we simply use (2.7) for E_f and this means considering only ordered wave energy, which is a choice, not an approximation.

It is convenient for the following analysis to introduce non-dimensional measures of both the wave energy flux $E_{f,w}$, the radiation stress and the energy dissipation. The following definitions are used.

$$B = E_{f,w} / (\rho g c H^2) \quad (2.9)$$

$$P = S_{xx} / \rho g H^2 \quad (2.10)$$

$$D = \mathcal{D}_t \cdot (4hT / \rho g H^3) \quad (2.11)$$

where T is the wave period and c the speed of propagation for the wave.

3. A CLOSED FORM SOLUTION TO THE ENERGY EQUATION

It turns out that the energy equation can be solved in closed form for a fairly general type of problem. With (2.11) and (2.7) substituted (2.4) reads

$$\frac{\partial E_{f,w}}{\partial x} = \rho g \frac{H^3}{4HT} D \quad (3.1)$$

The variation of the wave height is a combination of three effects: the change in water depth (which on a beach causes a wave height increase), the dissipation of energy (tending to reduce the wave height) and the change in shape of the wave (taken in a rather general sense) which is reflected in the variation of B, P and D.

Whereas the first two of these effects are represented in the time averaged equations, the same time averaging has excluded the possibility of assessing the change in wave shape (η , u , p , etc.) directly from the equations and the values of B, P and D must be evaluated separately (see sect. 5). Hence in the following we assume these parameters are known.

To obtain a solution to (3.1) we introduce a shoaling coefficient K_s defined so that at any depth

$$cB(K_s H_r)^2 = c_r B_r H_r^2 = \text{const} \quad (3.2)$$

where index $_r$ refers to some chosen reference point. This equation would give the H variation in the absence of dissipation. The actual wave height is then expressed as

$$H = K_s K_d H_r \quad (3.3)$$

which defines the dissipation coefficient K_d . Thus we get using (3.2) which implies $\partial/\partial x (cBK_s^2) = 0$:

$$\frac{\partial E_{f,w}}{\partial x} = 2\rho g K_d K'_d cBK_s^2 H_r^2 = 2E_{f,w} \cdot \frac{K'_d}{K_d}$$

(' denoting $\partial/\partial x$) which substituted into (3.1) yields

$$2 \frac{K'_d}{K_d} = \frac{HD}{4cBhT}$$

or

$$\frac{K'_d}{K_d^2} = \frac{K_s H_r D}{8cBhT}$$

or

$$\left(\frac{1}{K_d} \right)' = - \frac{K_s H_r D}{8cBhT} \quad (3.4)$$

So far no assumptions have been introduced neither about the type of wave considered (except that it is regular and progressive) nor about the nature of the energy dissipation. Thus (3.4) applies to waves in the surf zone as well as to the attenuation of waves due to bottom friction. (3.4) even applies to the growth of waves due to wind energy being added if we let $D > 0$. In the following, however, we concentrate on the surf zone where $D < 0$.

We now make the assumption (which will later be justified) that the coefficients on the right hand side only depend on the water depth h . (For a numerical evaluation of the following solution this assumption may be relaxed to include a weak dependence on H as well.) Hence (3.4) may be integrated directly giving

$$\frac{1}{K_d} = \frac{1}{K_{dr}} - \int_{x_0}^x \frac{K_s H_r D}{8cBhT} dx \quad (3.5)$$

where the integration constant is $K_{dr} = 1$ for $x_0 = x_r$. That is

$$K_d = \left[1 - \int_{x_r}^x \frac{K_s D H_r}{8cBhT} dx \right]^{-1} \quad (3.6)$$

Recalling that (3.2) implies

$$K_s = \left(\frac{c_r}{c} \frac{B_r}{B} \right)^{1/2} \quad (3.7)$$

we therefore get for H by substitution into (3.3)

$$\frac{H}{H_r} = K_s \left[1 - \frac{H_r}{8c_r B_r T} \int_{x_0}^x \frac{DK_s^3}{h} dx \right]^{-1} \quad (3.8)$$

We see that this closed form solution depends on one combination of the wave properties at the reference point, namely

$$\frac{H_r}{8c_r B_r T} = \frac{1}{8B_r} \frac{H_r}{h_r} \frac{h_r}{L_r} \quad (3.9)$$

(3.8), however, corresponds to a certain change in x . And since K_s mainly depends on h this means that the bottom slope h_x is actually a parameter as well. For monotonously changing depth we can express this explicitly by changing to h as integration variable. This yield

$$\left. \begin{aligned} \frac{H}{H_r} &= K_s \left[1 - K \int_{x_r}^x \frac{DK_s^3 h_{xr}}{h h_x} dh \right]^{-1} \\ \text{with} \quad K &\equiv \frac{1}{8B_r} \cdot \frac{H_r}{h_r} \cdot \left(\frac{h_x L}{h} \right)_r^{-1} ; \quad L \equiv cT \end{aligned} \right\} \quad (3.10)$$

and h_{xr} is h_x at the reference point. Hence the wave height variation in a surf zone will be the same for all wave conditions having the same value of K at the starting point of the computation (which, in principle, may be any point from the breaking point where D becomes non-zero and shorewards).

It also shows that the bottom slope itself is not a proper measure of the steepness of the beach. The relevant parameter is $h_x L/h$, which is the same slope parameter as was found for the shoaling of waves by Svendsen & Hansen (1976).

Notice that h includes the set-up, that is

$$h = h_{SWL} + \bar{\eta} \quad (3.11)$$

where h_{SWL} is the depth in the absence of waves.

4. ANALYTICAL SOLUTION FOR A SPECIAL CASE

One special case is of particular interest as it renders an analytical solution possible. It corresponds to a plane beach with D and B constant and $c = c_r \sqrt{gh}$. The latter assumption with c_r slightly larger than $\sqrt{gh_r}$ - and hence c slightly more than \sqrt{gh} but varying like $h^{1/2}$ - was found in I to be a good approximation.

In this case the integral in (3.10) may readily be solved and we get

$$\frac{H}{H_r} = \frac{1}{h'^{1/4} [1 + \frac{4}{3} KD(h'^{-3/4} - 1)]} \quad \text{with } h' = \frac{h + \bar{\eta}}{h_r} \quad (4.1)$$

In this solution is included the set-up $\bar{\eta}$ determined from the solution of the momentum equation. This, however, is nonlinear in $\bar{\eta}$ and not solvable except if $H/(h + \bar{\eta})$ is assumed constant (Bowen et al. (1968)). Although this is not realistic, for the major part of the surf zone, $\bar{\eta} \ll h$ and hence in evaluation (4.1) we may either completely neglect $\bar{\eta}$ (viz means $h' \sim (h/h_r)_{SWL}$) or use the above mentioned approximation $H/h = \alpha = \text{const.}$

The latter gives the approximation

$$\left. \begin{aligned} \bar{\eta} - \bar{\eta}_r &\sim \alpha_1 (h_{SWL} - h_{r,SWL}) \\ \alpha_1 &= \frac{2\alpha^2 P}{1 + 2\alpha^2 P} \end{aligned} \right\} \quad (4.2)$$

or (if we neglect $\bar{\eta}_r$ in comparison to h_r)

$$h' \sim \left(\frac{h}{h_r} \right)_{SWL} \cdot (1 + \alpha_1) - \alpha_1 \quad (4.3)$$

which differ from Bowen et al.'s result in that α is not assumed equal to 0.8.

Figs. 3
& 4

Figs. 3 and 4 show the variation of H/H_r and $H/h \cdot (H_r/h_r)^{-1}$ versus $h'_{SWL} = (h/h_r)_{SWL}$ for different values of KD and $\bar{\eta} = 0$.

In these figures we could, for example, consider the reference point taken at the breaking point.

Of particular interest is the variation of the wave height to water depth ratio H/h . As anticipated H/h is far from constant for any value of KD . For a wide range of KD , however, (which also turns out to be practically realistic) the H/h variation shows a minimum which may be recognized also in many experimental results (see e.g., Horikawa & Kuo (1966)).

Clearly this phenomenon reflects the basic feature mentioned above that the wave height variation is a balance between shoaling and dissipation. This can more readily be seen by writing (3.1) in the form (for derivation see I)

$$\left(\frac{H}{h}\right)_x = - \left[\frac{h_x}{h} + \frac{c_x}{2c} + \frac{B_x}{2B} \right] \frac{H}{h} + \frac{D}{8cTB} \left(\frac{H}{h}\right)^2 \quad (4.4)$$

The first bracket on the right side represents the shoaling, the last term the dissipation. Since at the reference (breaker) point H/h will usually be quite large, the second term will dominate provided $|D|$ is sufficiently large as in a breaker. Hence at a start $(H/h)_x$ is negative. As $(H/h)^2$ however decreases faster with H/h than does $(H/h)^1$ the difference between the two terms decreases till $(H/h)_x \sim 0$. Hence were it not for other effects H/h would asymptotically approach the value obtained by equating the right side to zero.

At the same time, however, as h decreases for constant h_x both h_x/h and c_x/c increases and near the shore line this effect becomes completely dominating resulting in the shown increase in H/h .

The position of the minimum for H/h can be found from (4.4) to be (with $c_x/c = h_x/2h$)

$$\left(\frac{H}{h}\right)_{\min} = 10 \frac{h_x L}{h} \frac{B}{D} \quad (4.5)$$

(Notice that both h_x and D are < 0 .) If we introduce K this becomes

$$\frac{(H/h)_{\min}}{(H/h)_r} = \frac{5}{4} (KD\sqrt{h'})^{-1} \quad (4.6)$$

which may be solved in combination with (4.1). The result is that the minimum for H/h occurs at

$$h'_{\min} = \left(\frac{8 KD}{20 KD - 15} \right)^{4/3}$$

This value and the corresponding value of H/h are shown in Fig. 5.

Fig. 5

We also see that for sufficiently small $KD (< 1.25)$ it turns out) the wave height will be increasing already from the reference point. This is not likely to happen for breakers but will sometimes be the situation where the dissipation is caused by bottom friction (that is seawards of the breaking point).

On the other hand, the situation may also occur that a wave approaching a shore will not break at all because its energy is being dissipated by bottom friction faster than the height can increase due to shoaling, so that it never

reaches a height sufficient for breaking to occur. Obviously this requires a very small bottom slope and we see from (3.10) that h_x small leads to K large so that even with the small D from bottom friction KD becomes larger than 1.25. (Fig. 4 also indicates that if breaking is to be avoided entirely then h_x must decrease shorewards. With constant h_x (however small) the wave height will start to increase sooner or later and hence the wave will reach breaking.)

The question, however, remains whether B , D and P can be considered constants through the surf zone (as assumed in this section), and what their values will be.

5. ENERGY FLUX, RADIATION STRESS AND ENERGY DISSIPATION IN THE SURF ZONE

The solutions derived above can theoretically be used right from the breaking point and shorewards, but it has often been pointed out (see e.g., I) that the flow in the so-called "outer region" immediately shoreward of the breaking point is significantly different from the conditions in the inner region. The transitions in the outer region will be discussed in Section 7.

First, however, values of the dimensionless parameters B , P and D are determined in the inner region.

The important feature dominating the wave motion in this region is the surface roller, which in essence is a volume of water carried shorewards with the breaker. Fig. 6 shows a typical situation, and also indicates a typical velocity distribution along a vertical at the front of the wave.

Fig. 6

The roller is defined as the recirculating part of the flow above the dividing streamline (in a coordinate system following the wave). Since it is resting on the front of the wave the absolute mean velocity in the roller equals the propagation speed c for the wave, and in the following we use this value for the velocity in the roller, neglecting the z -variation.

From this it follows that the roller represents a significant enhancement of the ordinary Stokes drift Q_s . Thus a surf zone wave potentially represents a much bigger mass transport than non-breaking waves. The actual net mass flux, however, is in any situation determined by the boundary conditions in the x -direction, and in the general three dimensional case it will also

depend strongly on the longshore variations of bottom topography and wave heights.

In the present two dimensional study we assume a zero net mass flux ($\bar{Q} = 0$), which of course implies that there is a return flow compensating for the surface drift.

From observations we know that in the inner region the change in wave shape is slow so the instantaneous volume flux

$$Q = \int_{-h}^{\eta} u(x, z, t) dz \quad (5.1)$$

may be determined as

$$Q = c\eta + \bar{Q} = Ud + \bar{Q} \quad (5.2)$$

where the surface profile is specified so that $\bar{\eta} = 0$. U is the wave particle velocity averaged over depth. As mentioned we shall further assume that $\bar{Q} = 0$.

Fig. 7

Although it is a crude simplification the velocity distribution shown in Fig. 7 will contain all the primary information outlined above and we will use that. The thickness e of the surface roller will be zero except in the front which is implicitly understood in the following derivations. Hence we get

$$Q = c\eta = ce + u_o(d-e) \quad (5.3)$$

Outside the roller we have

$$u_o = c(\eta - e)/(d - e) \quad (5.4a)$$

and in the roller

$$u = c \quad (5.4b)$$

The pressure in the wave motion is of course not static. In combination with the rather crude assumptions made above, however, it is consistent to assume a static pressure variation corresponding to the local, instantaneous position of the free surface. That is, using (2.3)

$$p_D = \rho g \eta \quad (5.5)$$

The Energy Flux B

With these assumptions we first calculate the non-dimensional energy flux B defined by (2.9). Substituted into (2.7) this yields (omitting the ~ which indicates the turbulent ensemble averaging)

$$B = \frac{1}{\rho g c H^2} \overline{\int_{-h}^{\eta} p_D + \frac{1}{2} \rho (u^2 + w^2) u dz} \quad (5.6)$$

Introducing the assumptions outlined above - which also implies neglecting the w^2 -contribution - we first get from (2.7)

$$E_{f,w} \approx \overline{\int_{-h}^{\eta} p_D u + \frac{1}{2} \rho u^3 dz} = E_{f,0} + E_{f,1} \quad (5.7)$$

where $E_{f,0}$ is the first term in the integral and $E_{f,1}$ the second. (5.5) gives

$$E_{f,0} = \overline{\int_{-h}^{\eta} p_D u dz} = \overline{\int_{-h}^{\eta} \rho g \eta u dz} \quad (5.8)$$

which by virtue of (5.2b) becomes

$$E_{f,0} = \rho g c \overline{\eta^2} = \rho g c H^2 \overline{(\eta/H)^2} \quad (5.9)$$

Thus the roller does not contribute to this term. For $E_{f,1}$ we get

$$E_{f,1} = \frac{1}{2} \rho \left[\int_{-h}^{\eta-e} u_o^3 dz + \int_{\eta-e}^{\eta} c^3 dz \right] \\ \approx \frac{1}{2} \rho g c H^2 \frac{H}{h} \cdot \overline{\left(\frac{\eta}{H} \right)^3} + \frac{1}{2} \rho c^3 \frac{1}{T} \int_0^T edt \quad (5.10)$$

where $c^2 \sim gh$ and $\eta \ll h$ has been used in the first term. Since $\bar{\eta} = 0$ we will find that $\overline{(\eta/H)^3} \ll \overline{(\eta/H)^2}$, the latter being an integral of a non-negative quantity (see Hansen, 1980).

The area A of the surface roller is defined as

$$\int_0^T edt \approx \frac{1}{c} \int_0^\lambda edx = \frac{A}{c} \quad (5.11)$$

where λ is the length of the roller (see Fig. 6). In (5.10) this yields

$$E_{f,1} \approx \frac{1}{2} \rho c^3 \frac{A}{L} \approx \frac{1}{2} \rho g H^2 c \cdot \frac{A}{H^2} \frac{h}{L} \quad (5.12)$$

which shows that the contribution to the energy flux from the surface roller is proportional to its area in the vertical plane.

Very little information is available about the size of the surface roller. Duncan (1981) has measured A in a breaker behind a towed hydrofoil, and his results are shown in Fig. 8. For the present application we will approximate these results with

$$A \sim 0.9 H^2 \quad (5.13)$$

and hence we get for $E_{f,w}$

$$E_{f,w} \approx \rho g c H^2 \left[\overline{\left(\frac{\eta}{H} \right)^2} + 0.45 \frac{h}{L} \right] \quad (5.14)$$

Fig. 8

and from (5.6) for B

$$B = \frac{1}{T} \int_0^T \left(\frac{\eta}{H} \right)^2 dt + \frac{1}{2} \frac{A}{H^2} \frac{c^2}{gL} \approx \frac{1}{T} \int_0^T \left(\frac{\eta}{H} \right)^2 dt + 0.45 \frac{h}{L} \quad (5.15)$$

Here L is a local quantity defined as cT , not the physical distance between two consecutive wave crests.

Values of B_o defined as

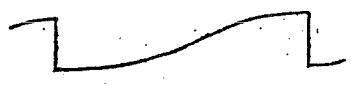
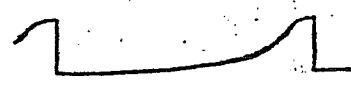


$$B_o = \frac{1}{T} \int_0^T \left(\frac{\eta}{H} \right)^2 dt$$

are shown for waves in the surf zone in Fig. 9. The measurements are all taken on a 1/34.3 slope at ISVA and the results only show the trend in the variation. Clearly there is a significant amount of scattering but also some systematic variation with wave parameters (such as the deep water steepness H_o/L_o) which needs further documentation and analysis.

The main tendency, however, is quite obviously that from the point of breaking B_o increases rapidly from a relatively small value (indicating a rather peaky wave profile representing a small energy flux for a given wave height) towards values around 0.07 - 0.08. The variation may be further illustrated by the examples given in Table 1 for some simple surface profiles. Of particular interest are the value 0.083 and 0.089 for triangular and parabolic wave shapes respectively, because surf zone wave profiles often resemble such shapes as Fig. 10 shows.

Fig. 10

Table 1

	$\frac{\eta}{H} = \sin \frac{\pi t}{T}$	$B_o = 0.125 = \frac{1}{8}$
	cnoidal	any $B_o < \frac{1}{8}$
	$\frac{\eta}{H} = \left(\frac{t}{T}\right)^2 - \frac{1}{3}$	$B_o = 0.089$
	$\frac{\eta}{H} = \frac{t}{T} - \frac{1}{2}$	$B_o = 0.083 = \frac{1}{12}$

The Radiation Stress P

The radiation stress defined by (2.2) represents the time averaged momentum flux. In (2.2) is included the effect of the turbulent normal stresses as well as any net volume flux superimposed on the wave.

The latter, however, we are excluding here. The contribution from the turbulent stresses was analysed by Stive & Wind (1982) on the basis of experimental data. They concluded that this effect only increases the radiation stress by some 5%. Part of the reason for this modest effect of strong turbulence is that the vertical velocity fluctuations reduce the pressure whereas the horizontal fluctuations increase the momentum flux. Hence in the present context we may neglect the turbulent contribution to S_{xx} .

Using (5.5) we then get for F_p in (2.2)

$$F_p = \int_{-h}^{\eta} \rho g \eta dz - \frac{1}{2} \rho g \overline{\eta^2} = \frac{1}{2} \rho g \overline{\eta^2} \quad (5.17)$$

which by means of (5.16) may be written

$$F_p = \frac{1}{2} \rho g H^2 B_o \quad (5.18)$$

For F_m we get, using (5.4a,b)

$$F_m = \int_{-h}^{\eta} \rho u^2 dz = \rho \left(\overline{u_o^2 (d-e)} + \overline{c^2 e} \right) \quad (5.19)$$

Here

$$\overline{u_o^2 (d-e)} = c^2 \left(\frac{\overline{\eta^2 - 2\eta e + e^2}}{d - e} \right) \quad (5.20)$$

which we approximate by using $e \ll d$. We also notice that since $e \neq 0$ almost symmetrically around $\eta = 0$ the value of $\overline{\eta e}$ must be very small. Hence we get

$$F_m \sim \rho c^2 \left(\frac{\overline{\eta^2}}{d} + \frac{\overline{e^2}}{d} + \overline{e} \right) \sim \rho \frac{c^2}{h} H^2 \left(\left(\frac{\overline{\eta}}{H} \right)^2 + \left(\frac{\overline{e}}{H} \right)^2 + \frac{\overline{eh}}{H^2} \right) \quad (5.21)$$

From Duncan's results can be found that $e/H \sim 0.3$ and since $e = 0$ over most of the wave profile it follows that $\overline{(e/h)^2} \ll \overline{(\eta/H)^2}$ so that we for F_m get (again using $c \sim \sqrt{gh}$)

$$F_m \sim \rho g H^2 \left(B_o + \frac{A}{H^2} \frac{h}{L} \right) \quad (5.22)$$

In combination with (5.18) and (5.13) this yields for S_{xx}

$$S_{xx} = \rho g H^2 \left(\frac{3}{2} B_o + 0.9 \frac{h}{L} \right) \quad (5.23)$$

or

$$P = \frac{3}{2} B_o + 0.9 \frac{h}{L} \quad (5.24)$$

With the results from Fig. 9 for B_o and a typical value of 0.05 - 0.10 for h/L we see that the presence of the surface roller roughly doubles the radiation stress.

The Energy Dissipation D

The third parameter in the equations is the dimensionless energy dissipation D. A detailed analysis of D is quite complicated and is considered unnecessary in combination with the simplifying assumptions introduced at a number of other points. Svendsen & Madsen (1981) showed that neglecting the form change the energy dissipation in a surf zone wave can be determined by

$$\frac{D}{D_{\text{bore}}} = 1 + \frac{\zeta+1}{(\zeta-1)^2} \frac{(\beta_t - \alpha_t)\zeta^2 + (\alpha_c - \alpha_t)\zeta - (\beta_c - \alpha_t)}{\alpha_t\zeta - \alpha_c} \quad (5.25)$$

where α , β are coefficients for depth averaged velocity and pressure contributions in the momentum and energy equations, and $_t$ and $_c$ refer to trough and crest respectively. With the assumptions outlined above, however, this expression simplifies to

$$D = D_{\text{bore}} \quad (5.26)$$

where D_{bore} is the energy dissipation in a bore of the same height as the wave. The dimensional form of D_{bore} is ($\zeta = d_c/d_t$)

$$\Delta E = \rho g Q d_t \frac{(\zeta-1)^3}{4\zeta} \quad (5.27)$$

(see e.g., Henderson (1966)). In a wave $Q \equiv u_t d_t = ch$ so this may also be written

$$\Delta E = \rho g ch \frac{H^3}{4d_t d_c} \quad (5.28)$$

If we assume that each breaker suffers a similar dissipation per second then the mean dissipation per m^2 bottom area is $\Delta E/L$. And substituting

this for \mathcal{D}_t in (2.11) then yields

$$D = \frac{h^2}{d_t d_c} \quad (5.29)$$

Introducing the crest elevation η_c instead of d_c and d_t we get

$$d_c = h + \eta_c \quad ; \quad d_t = h + \eta_c - H \quad (5.30)$$

and thus

$$D = \left[\left(1 + \frac{\eta_c}{H} \frac{H}{h} \right) \left(1 + \frac{H}{h} \left(\frac{\eta_c}{H} - 1 \right) \right) \right]^{-1} \quad (5.31)$$

which shows that for fixed η_c/H D does depend slightly on H/h . Fig. 11 shows the variation and Fig. 12 gives values of η_c from the experiments quoted above. As was the case for B_o the results for η_c/H show significant scattering but in the inner region of the surf zone the value is mostly 0.6 - 0.7 which from Fig. 11 is seen to represent a D nearly independent of H/h .

Fig. 11 also shows that D only varies slightly with η_c/H . In other words, the primary variation of the energy dissipation is represented by the H^3/h dependency already accounted for in the definition (2.11).

6. COMPARISON WITH MEASUREMENTS

The outer and the inner region

The original concept of an outer (transition) region and an inner (bore) region was primarily based on the visual observations of wave behaviour after breaking (see I). The impression is one of a gradual change towards the bore shape found in the inner region. Consequently no attempt was made to define a proper limit between the two regions and wave height measurements truly do not suggest a natural definition.

The situation is quite different when the variations in mean water level are considered. Fig. 13 shows some examples from Hansen & Svendsen (1979) covering a wide range of deep water steepnesses. They all exhibit a marked change in the slope of the mean water level at some distance shoreward from the breaking point. A similar variation can also be seen in other investigations such as Bowen et al. (1968) and Stive & Wind (1982). The mean water level is horizontal or weakly sloping over a distance of 5-8 times the breaker depth and then a rather sharp increase in slope occurs. The distance of nearly horizontal mean water level is comparable to the distance of the most obvious transformations of the wave shape following after the initiation of breaking, and so it will be coherent with the original concept to define the limit between the outer and the inner region as the point where the slope of the mean water level changes. In the following this is termed the transition point.

Wave conditions in the inner region

Physical explanations for these changes are sought in section 7.

First, however, we notice that since the results derived above for the parameters B, P and D are based on the wave properties in the inner zone comparisons with experimental data should start in that region. It is convenient to use the same reference point in all computations. To start computations at the above defined transition point (and emphasize the arbitrariness of the reference point) we therefore write (3.6) as

$$\frac{1}{K_d} = 1 - \frac{H_r}{8c_r B_r T} \left[\int_{h_r}^{h_t} \dot{dh} + \int_{h_t}^h dh \right] \frac{DK_s^3}{hh_x} \quad (6.1)$$

which upon definition of

$$\frac{1}{K_t} = 1 - \frac{H_r}{8c_r B_r T} \int_{h_r}^{h_t} \frac{DK_s^3 dh}{hh_x} \quad (6.2)$$

can be written

$$\frac{1}{K_d} = \frac{1}{K_t} - \frac{H_r}{8c_r B_r T} \int_{h_t}^h \frac{DK_s^3}{hh_x} dh \quad (6.3)$$

(which can also be obtained directly from (3.5)). For the wave height this means

$$\frac{H}{H_r} = (c'B')^{-1/2} \left[\frac{1}{K_t} - K \int_{h_t'}^{h'} \frac{Ddh'}{(c'B')^{3/2} h'} \right]^{-1} \quad (6.4)$$

where we in analogy to (4.1b) have defined

$$c' = c/c_r \quad ; \quad B' = B/B_r \quad (6.5)$$

K is given by (3.10b) and K_t by (6.2) which can also be written (see (3.3) and (3.7))

$$K_t = \frac{H_t}{H_r} / K_{st} = \frac{H_t}{H_r} (c'_t \cdot B'_t)^{1/2} \quad (6.6)$$

In all these expressions index $_t$ indicates values at the transition point.

Using this (slightly more general) version of the solution derived in section 3 we are still free to let the reference point also be, for example, the transition point. In the following computations, however, and the corresponding figures we have chosen the breaker point (B) as reference.

The momentum equation (2.1) is solved simultaneously with the determination of the wave height. Hence (3.11) is used for h in (6.4). With (2.10) and (5.24) substituted (2.1) becomes

$$\frac{d\bar{\eta}}{dx} = \frac{1}{h+\bar{\eta}} \frac{d}{dx} \left[\left(\frac{3}{2} B_o + 0.9 \frac{h}{L} \right) H^2 \right] \quad (6.7)$$

In the computations we neglect the variation of B_o and assume that $h/L \propto \sqrt{h'}$. It is emphasized again that this means c is proportional to \sqrt{gh} , not equal to (see I). For B_o and η_c is used $B_o = 0.075$ (see Fig. 9) and $\eta_c/H = 0.6$ (Fig. 12).

Discussion of results

Figs. 14, 15 and 16 show a comparison with results for three rather different wave steepnesses, all on a plane slope 1/34.3. In general the agreement is quite good particularly for the set-up. The latter is of particular interest because the calculations show that $\bar{\eta}$ is much more sensitive to the assumptions made than is the wave height variation. As can be expected from what was said above the H variation is virtually independent of the choice of η_c/H .

It is noticed that in some of the cases the H -variation is slightly less curved than corresponding to the best fit of measurements, and the values of H grow a little too large. This tendency will be further amplified if a larger value for η_c/H is used (see Figs. 11 and 12). Both these points can be adjusted by using a value of D perhaps 20-30% larger than given by (5.31), which is quite consistent with the results reported earlier (see I and Svendsen & Madsen, 1981) that the actual energy dissipation in a surf zone wave is larger than in a hydraulic jump of the same height.

The effect of including the surface roller in B can be understood by considering the energy equation in the form (4.4). In the first bracket representing the shoaling mechanism B_x/B is much smaller than the other two terms. So the value of B mainly enters the last term. Hence the increase in B due to the roller is equivalent to a similar decrease in D , and the observation above that D is too small could also be due to an overestimation of B .

In Figs. 14-16 are also included results obtained by omitting the surface roller (dotted curve corresponding to $B = B_0$ and $P = 3/2 B_0$). The effect is quite appreciable. On the other hand, considering that the presence of the surface roller nearly doubles energy flux and radiation stress the difference between the full and the dotted lines in these figures indicates that the effect of also including turbulence, deviation from static pressure, etc. would hardly be discernible.

The strongest justification, however, for the importance of the surface roller is obtained by considering the motion in the transition region.

7. THE WAVE MOTION IMMEDIATELY AFTER BREAKING

It is tempting and illustrative first to try if the solution presented in the previous chapters also applies to the region of rapid transition right after the initiation of breaking.

Fig. 17 shows a computation of the wave height variation, starting at the breaking point. The agreement is surprisingly good. (Again either D is slightly too small or B too large.) This, however, does not apply to Fig. 18, which gives a similar comparison for the set-up $\bar{\eta}/h_{MWS}$. The two figures together show the paradoxical fact already hinted at earlier that the radiation stress in the transition region stays nearly constant even with a 30-40% decrease in wave height. Recalling (2.10) this can only be true if P is increasing, roughly as H^{-2} .

By considering what happens when the breaking starts, it becomes clear that the collapse of the wave cannot immediately be matched by dissipation of a similar amount of energy. In the first transformation a large amount of the lost potential energy is converted into forward momentum flux which eventually is concentrated mainly in the roller, and this must be the reason for the simultaneous increase in P .

This is also consistent with the fact that P for very high waves is rather small. There are no results available for the skew waves at the breaking point, but the high order results for Stokes waves presented by Cokelet (1977) can be used to determine P for very high, symmetrical waves. Fig. 19 shows the variation of P with H/h for two values of h/L . Notice that for the highest

waves P is less than half the value of $3/16$ for linear long waves and considerably less than P for cnoidal waves of the same height.

The increase in P , however, is inevitably associated with a similar increase in B , the energy flux for a wave of unit height and propagation speed. The problem is the same as for P : very steep waves with peaky crests represent a very small energy flux relative to their height (Fig. 20 shows results similar to those for P) and the collapse of the crest in the initial stage of breaking leads to a significant increase in B .

As we will see shortly these shifts in P and B are also consistent with the result found in Chapter 5, that waves in the inner region represent rather high values of radiation stress and energy flux relative to their height and speed.

But even with no energy dissipation an increase in B will in itself require a decreasing wave height. Hence the question arises: how much of the wave height decrease in the outer transition region is actually due to redistribution of energy (represented by the changes in P and B) and how much is real energy dissipation?

This problem and the change in B and P can be analysed by considering the conservation of momentum and energy over the transition region as a whole in analogy to the jump conditions that applies to bores and hydraulic jumps in open channel flow and to shocks in compressible flows.

Between the breaking point (denoted with suffix $_B$) and the transition point ($_t$) we have from (2.8)

$$E_{f,t} - E_{f,B} = \int_0^{\ell} \mathcal{D} dx = \mathcal{D}_1 \quad (7.1)$$

where ℓ is the width of the transition region. We are interested in determining how large a fraction \mathcal{D}_1 is of the energy dissipation we would have had, had B stayed constant and equal to B_B . This energy dissipation would obviously have been

$$\mathcal{D}_m = \rho g B_B (c_t H_t^2 - c_B H_B^2) = E_{fB} \left(\sqrt{h'_t} \left(\frac{H_t}{H_B} \right)^2 - 1 \right) \quad (7.2)$$

by virtue of (2.9). Using (2.9) in (7.1) as well yields

$$\mathcal{D}_1 = E_{fB} \left(\sqrt{h'_t} \left(\frac{H_t}{H_B} \right)^2 \frac{B_t}{B_B} - 1 \right) \quad (7.3)$$

so that the ratio we are looking for is

$$\Delta = \frac{\mathcal{D}_1}{\mathcal{D}_m} = \frac{a B_t/B_B - 1}{a - 1} \quad a \equiv \sqrt{h'_t} \left(\frac{H_t}{H_B} \right)^2 \quad (7.4)$$

In the momentum equation (2.1) we have $\partial \bar{\eta} / \partial x \approx 0$ and hence, using (2.10)

$$P_t = P_B (H_B/H_t)^2 \quad (7.5)$$

Finally since P_t and B_t are given by (5.24) and (5.15), respectively, we have by elimination of B_0 between those two

$$B_t = \frac{2}{3} P_t - 0.15 \sqrt{h'_t} h_B / L_B \quad (7.6)$$

Thus if we know the properties of the wave at breaking we can determine B_t , P_t and Δ . In need of more correct information we use (from Figs. 19 and 20) for an example with $h_B/L_B = 0.057$

$$B_B = 0.05 \quad , \quad P_B = 0.07$$

and assume the transition point is at $h'_t = 0.85$ with $H_t/H_B = 0.65$. We then get from (7.4)

$$\Delta = 0.33 \quad ;$$

which means that only 33% of the energy that corresponds to the decrease in wave height is actually lost. The increase in B accounts for the rest. We further get

$$(7.5): \quad P_t = 0.166 \quad \text{against (5.24):} \quad P_t = 0.152$$

$$(7.6): \quad B_t = 0.103 \quad \text{against (5.15):} \quad B_t = 0.094$$

Thus the value of P_t and B_t required to account for the gross change in the radiation stress/mean water level and the wave height over the transition region agrees well with the values we can determine for a wave at the start of the bore region using the ideas from section 5.

This is taken as another indication that the ideas presented in that section for the properties of waves in the inner region are at least qualitatively correct.

As mentioned above the constant radiation stress in the transition region must imply

$$P \propto H^{-2} \quad (7.7)$$

Most measurements further show that H varies approximately linearly, i.e.,

$$H \propto H_b - \alpha x \quad (7.8)$$

after breaking. Since the variation of H is much faster than the variation in depth, and since $E_f \propto \sqrt{h} H^2$ we may neglect c_x in (2.8) and write

$$\frac{1}{E_f} \frac{dE_f}{dx} \approx \frac{B_x}{B} - \frac{2\alpha}{H} = \frac{DH}{4hLB} \quad (7.9)$$

However if we in this equation - in analogy with the situation in the bore region represented by (7.6) - assume that $B \propto P + \text{const}$, then (7.9) yields $D = 0$ which clearly is not correct. Hence (7.9) is not suitable for assessing D on the basis of some reasonable conjecture for B .

So if one wants to be able to extend the method described in this paper to the transition region there is room for both further experimental investigations and for some empirical interpolation formulas for the development of D from zero at the breaking point to the value given by (5.31) at the transition point.

In the absence of such results there is always the possibility of using (7.7) for P in the transition region to get the correct $\bar{\eta}$ -variation and let B and D be given by the bore values (5.15) and (5.31) right from the breaking point (which we have seen will give approximately the correct H -variation). It is just that this means B is discontinuous at the breaking point (which, of course is not true) and it is also an unsatisfactory procedure from a physical point of view because it obviously does not model the real processes.

8. SUMMARY AND CONCLUDING REMARKS

The physical mechanisms behind the variation of wave heights and set-up in the surf zone have been analysed and a theoretical model has been suggested. It is based on rather simple approximations for the integral properties of the wave motion. Comparison in the inner region of the surf zone with experiments shows acceptable agreement.

An attempt has been made to explain the nature of the transformations of the waves in the transition zone right after breaking (Section 7).

The methods for determining the non-dimensional energy flux B , radiation stress P and energy dissipation D can easily be refined, the crest elevation η_c/H may perhaps more correctly be determined by a linearly decreasing function, etc. Such improvements, however, are not likely to change the basic conclusion that the major difference between surf zone waves and ordinary waves is represented by the surface roller. And as a first approximation the roller can be considered as a volume of water carried shoreward with the wave. This picture is found to be in accordance both with the motion alleged for the inner region and with the changes occurring over the transition region.

The author gratefully acknowledges access to the unpublished data sent by J. Buhr Hansen and used in some of the figures.

REFERENCES

- BOWEN, A. J., D. L. INMAN & V. P. SIMMONS (1968). Wave 'set-down' and wave set-up. *J. Geophys. Res.*, 73, 2569.
- COKELET, E. D. (1977). Steep gravity waves in water of arbitrary uniform depth. *Phil. Trans. Roy. Soc. Lond.*, 286, 183-230.
- DIVOKY, D., B. LEMEHAUTÉ & A. LIN (1968). Breaking waves on gentle slopes. *Jour. Geophys. Res.*, 75, 1681-1692.
- DUNCAN, J. H. (1981). An experimental investigation of breaking waves produced by a towed hydrofoil. *Proc. Roy. Soc. Lond.*, A 377, 331-348.
- HANSEN, J. B. (1980). Experimental investigations of periodic waves near breaking. *Proc. 17 Coast. Engrg. Conf.*, Sydney, 260-277.
- HANSEN, J. B. (1982). Wave measurements in the surf zone. Private communication of unpublished data.
- HANSEN, J. B. & I. A. SVENDSEN (1979). Regular waves in shoaling water, experimental data. *Inst. Hydrodyn. & Hydr. Engrg. Series Paper 21*.
- HENDERSON, F. M. (1966). Open channel flow. Macmillan Publ. Co., N.Y., 522 pp.
- HORIKAWA, K & C. KUO (1966). Wave transformation after breaking point. *10th Conf. Coast. Engrg.*, Tokyo, 217-233.
- JAMES, I. D. (1974). Non-linear waves in the nearshore region: Shoaling and set-up. *Estuarine Coastal Mar. Sci.*, 2, 207-234.
- LEMEHAUTÉ, B. (1962). On the non-saturated breaker theory and the wave run-up. *Proc. 8th Coast. Engrg. Conf.*, 77-92.

STIVE, M. J. F. (1980). Velocity and pressure field of spilling breakers.

Proc. 17th Coast. Engrg. Conf., Sydney, 547-566.

STIVE, M. J. F. & H. G. WIND (1982). A study of radiation stress and set-up in the nearshore region. Coastal Engineering, 6, 1-25.

SVENDSEN, I. A. & J. B. HANSEN (1976). Deformation up to breaking of periodic waves on a beach. Proc. 15th Coast. Engrg. Conf., Honolulu, Chap. 27, 477-496.

SVENDSEN, I.A., P. A. MADSEN & J. B. HANSEN (1978). Wave characteristics in the surf zone. Proc. 16th Coast. Engrg. Conf., Hamburg, I, Chap. 29, 520-539.

SVENDSEN, I. A. & P. A. MADSEN (1981). Energy dissipation in hydraulic jumps and breaking waves. Progr. Rep. 55, Inst. Hydr. & Hydraulic Engrg., 39-47.

WANG, H. & W-C. YANG (1980). A similarity model in the surf zone. Proc. 17th Coast. Engrg. Conf., Sydney, 529-546.

LIST OF CAPTIONS

1. Regions in the surf zone (from I).
2. Definitions.
3. H/H_r from analytic solution (4.1) versus $(h/h_I)_{MWS}$.
4. $\frac{H}{h} \left(\frac{H_r}{h_r} \right)$ from analytic solution versus $(h/h_I)_{MWS}$.
5. Minimum values of $H/h_{SWL}/(H_r/h_r)$ and the value h'_{min} of h' at which they occur.
6. The roller of a surf zone wave.
7. The approximation for the horizontal velocity profile.
8. Cross section area A for a roller. Measurements by Duncan (1981).
9. Measured values of B_o defined by (5.16). (Data from Hansen, 1982).
10. Wave profiles in the surf zone. Derived from measurements in I.
11. The variation of D with H/h and η_c/H according to (5.31).
12. Measurements of η_c/H in the surf zone. (Data from Hansen, 1982).
13. Measurements of the mean water level shoreward of the breaking point.
Also shown is the value of local wave height to breaker height, H/H_B .
(Measurements from Hansen & Svendsen, 1979).

14. Wave heights and set-up for a wave with deep water steepness $H_o/L_o = 0.071$.
 ——— Theory using (6.4) and (6.7).
 • Measurements by Hansen & Svendsen (1979), Case B.

15. Wave heights and set-up for a wave with deep water steepness $H_o/L_o = 0.024$.
 ——— Theory using (6.4) and (6.7).
 • Measurements by Hansen (1982), Case H.

16. Wave heights and set-up for a wave with deep water steepness $H_o/L_o = 0.0107$.
 ——— Theory using (6.4) and (6.7).
 • ~~Measurements~~ by Hansen & Svendsen (1979), Case N.

17. Wave height using (6.4) and (6.7) from the breaking point.
 Measurements by Hansen (1982), Case H.

18. Set-up using (6.4) and (6.7) from the breaking point.
 Measurements by Hansen (1982).

19. The non-dimensional radiation stress for symmetrical waves.
 ——— Results from Cokelet (1977), - - - lowest order cnoidal waves.

20. The non-dimensional energy flux in symmetrical waves.
 ——— Results from Cokelet (1977), - - - lowest order cnoidal waves.

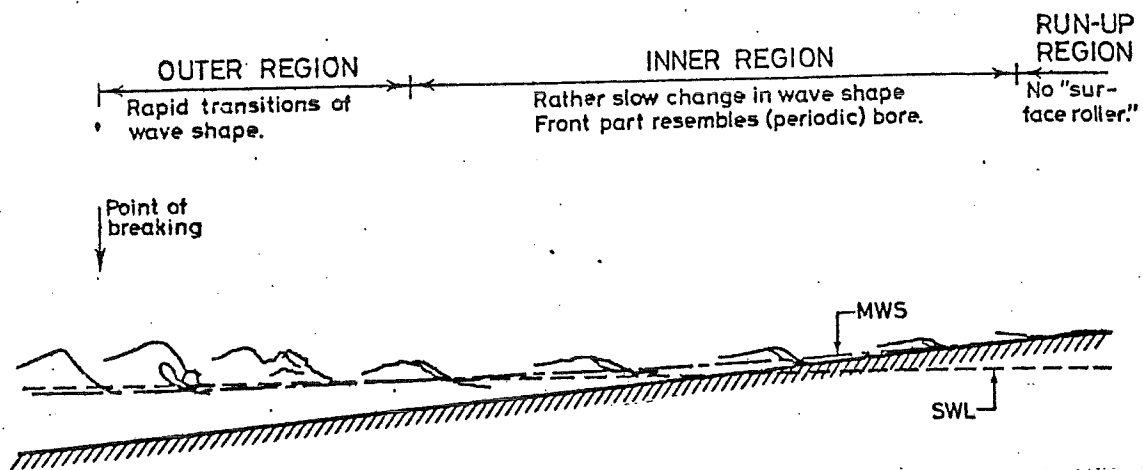


Fig 1

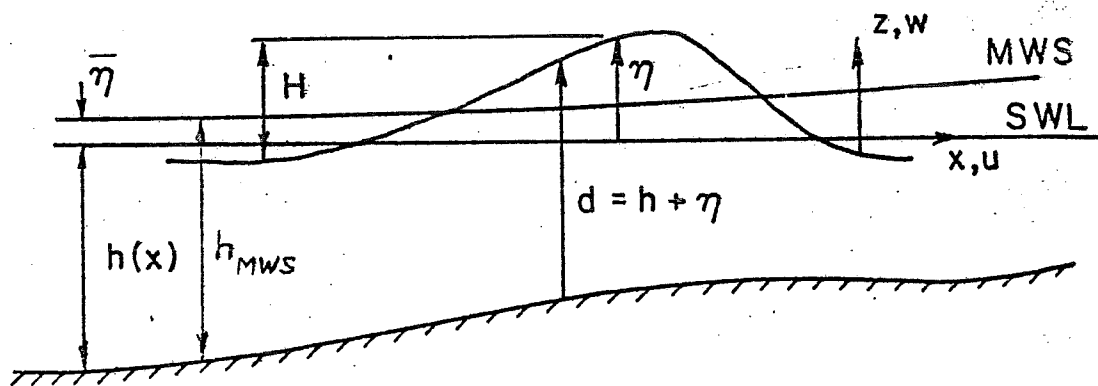


Fig 2

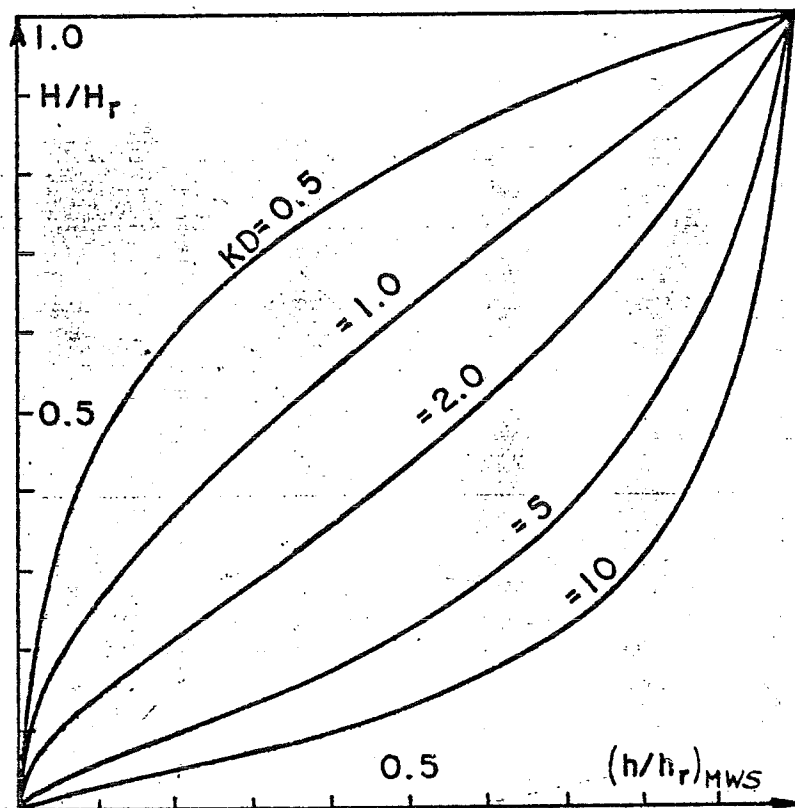


Fig 3

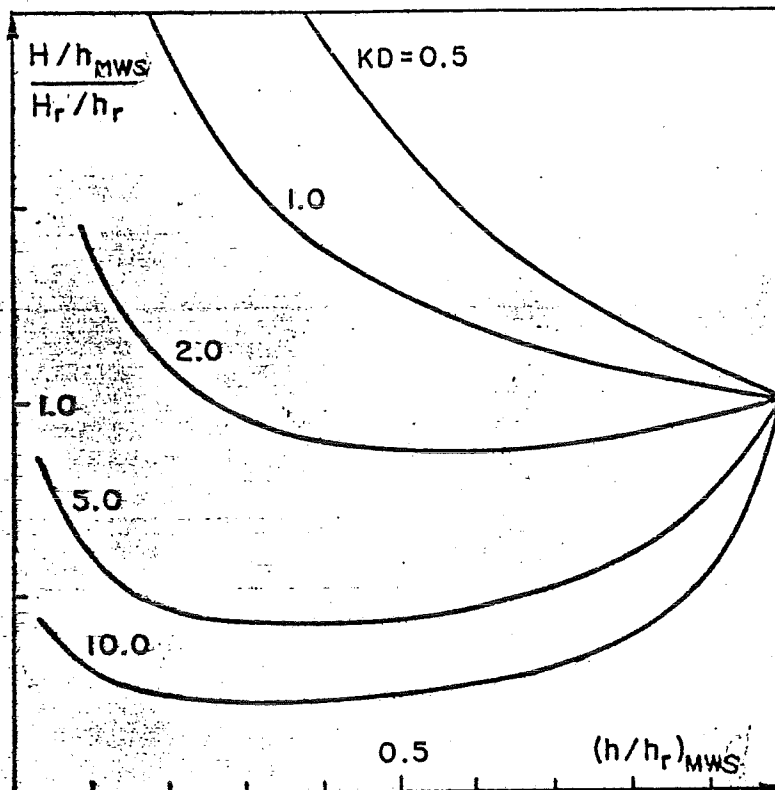


Fig 4

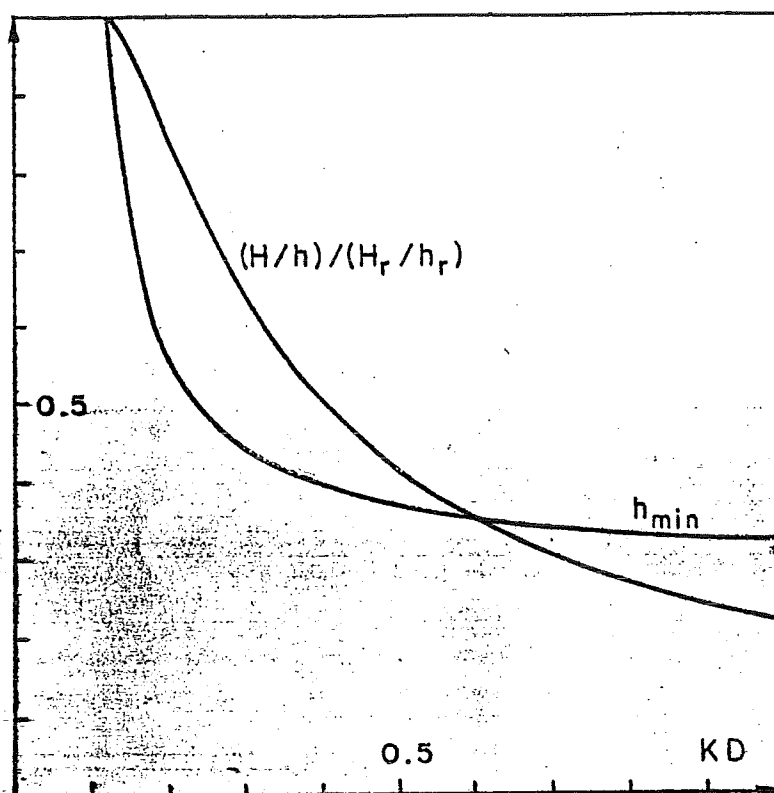


Fig 5

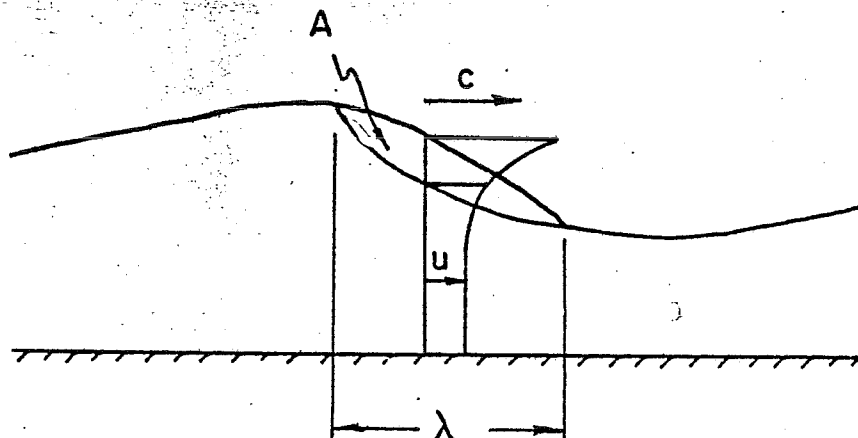


Fig 6

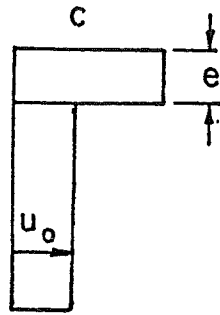


Fig. 7

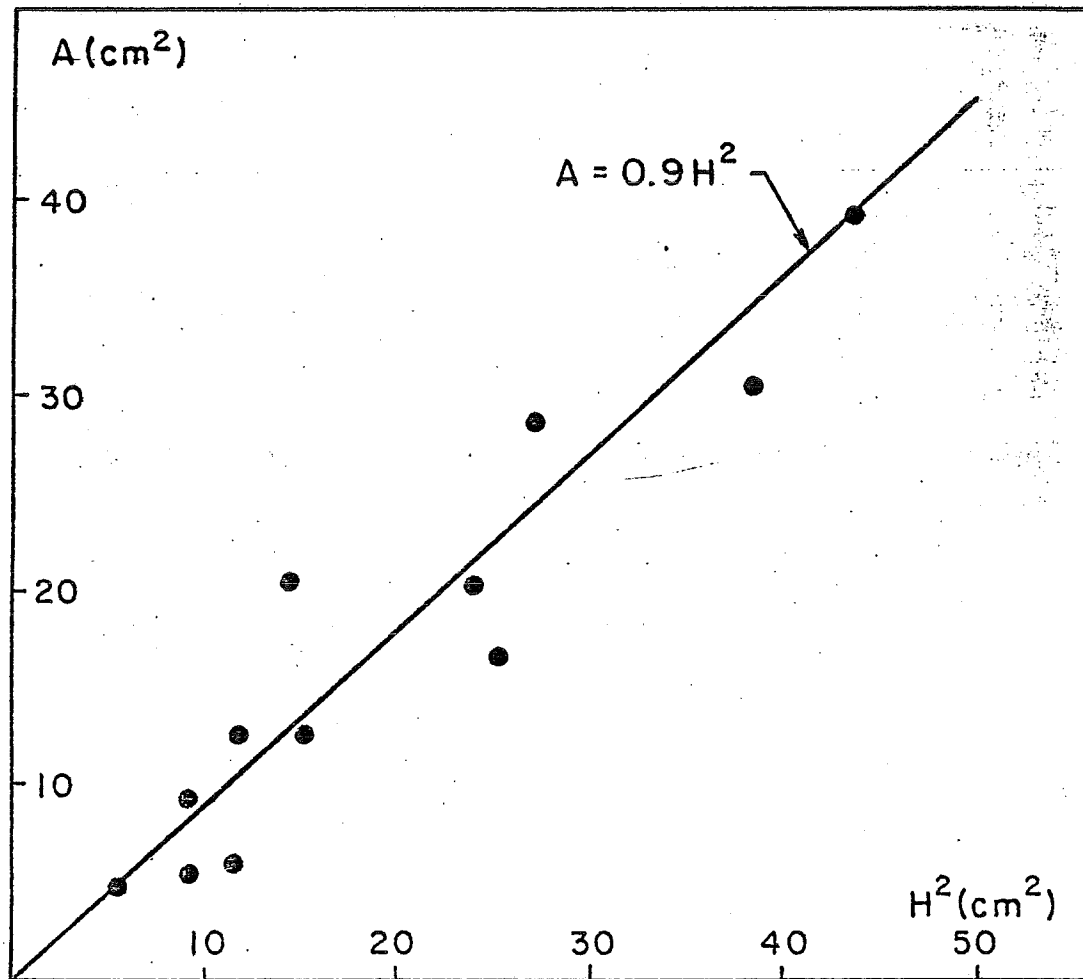
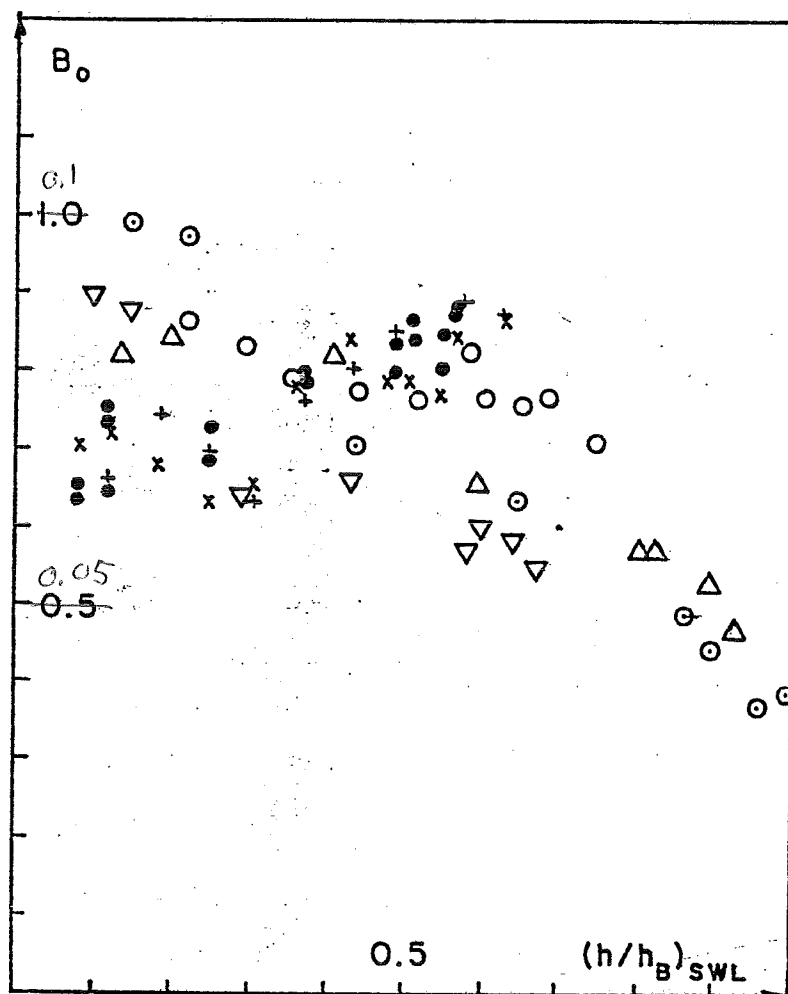


Fig 8



	H_0/L_0
•	~ 0.034
x	~ 0.034
○	~ 0.0093
△	~ 0.003
▽	~ 0.0053
○	~ 0.0053
+	~ 0.034

Fig 9

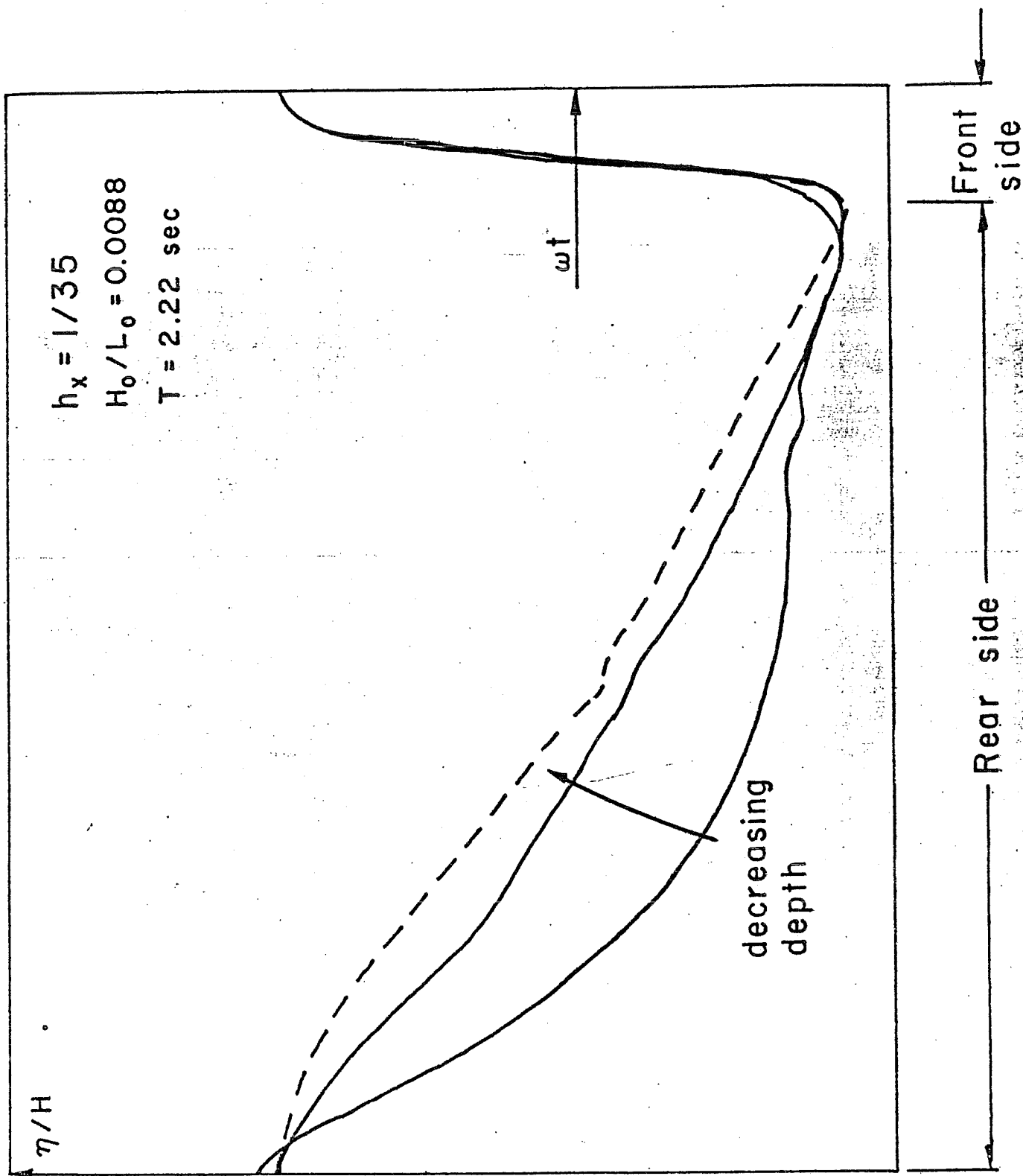


Fig 10 a

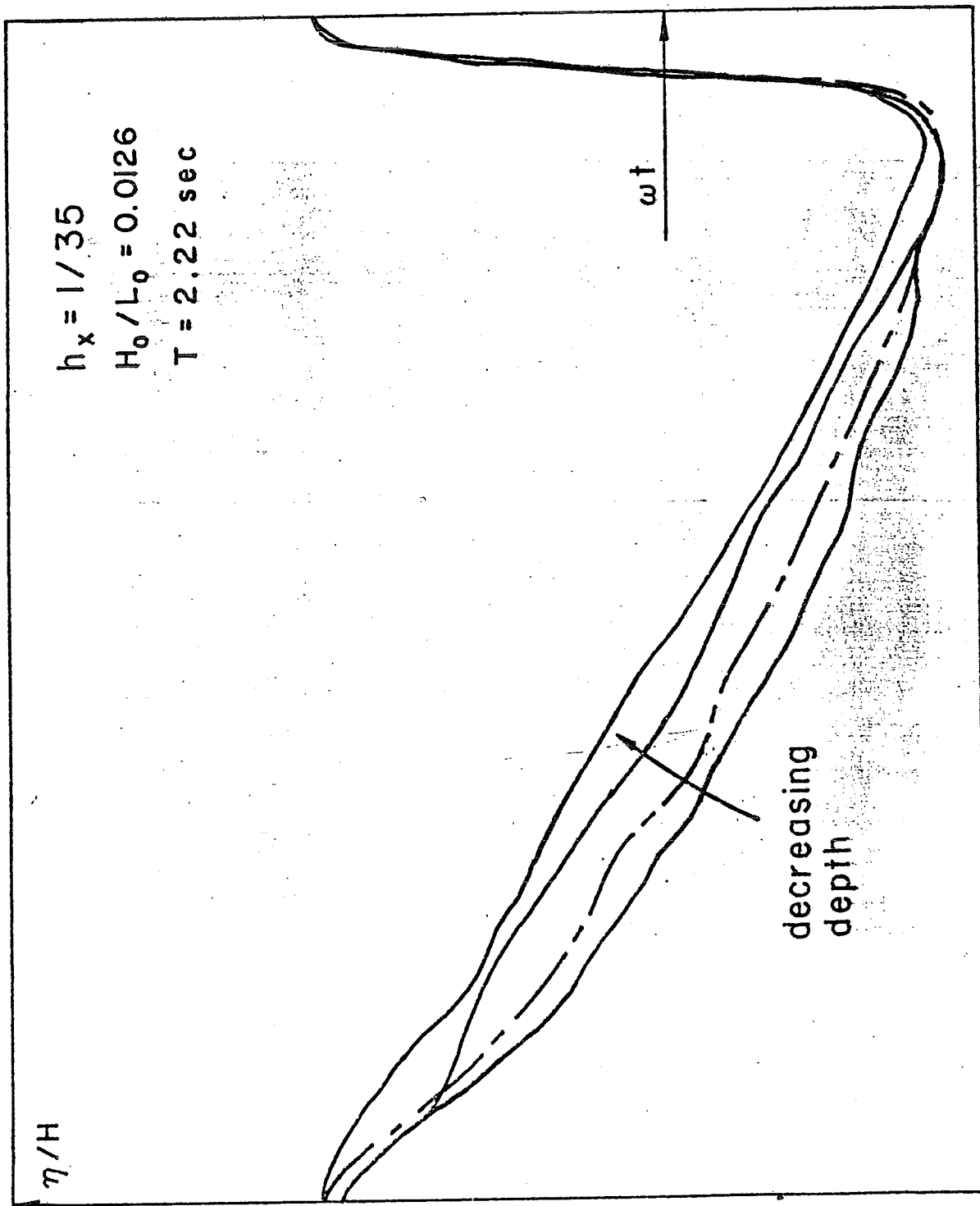


Fig 10b

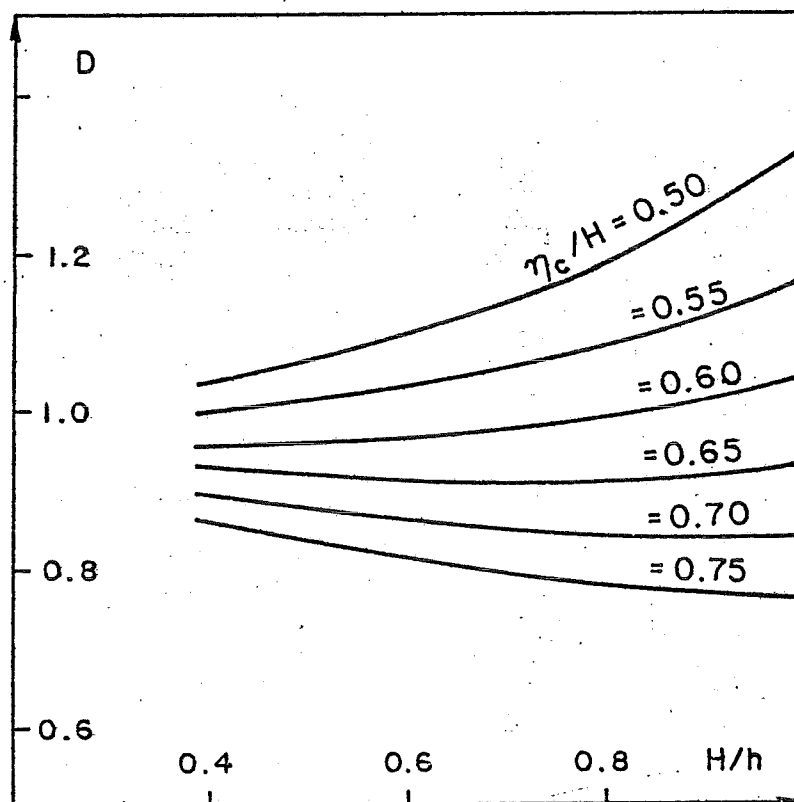
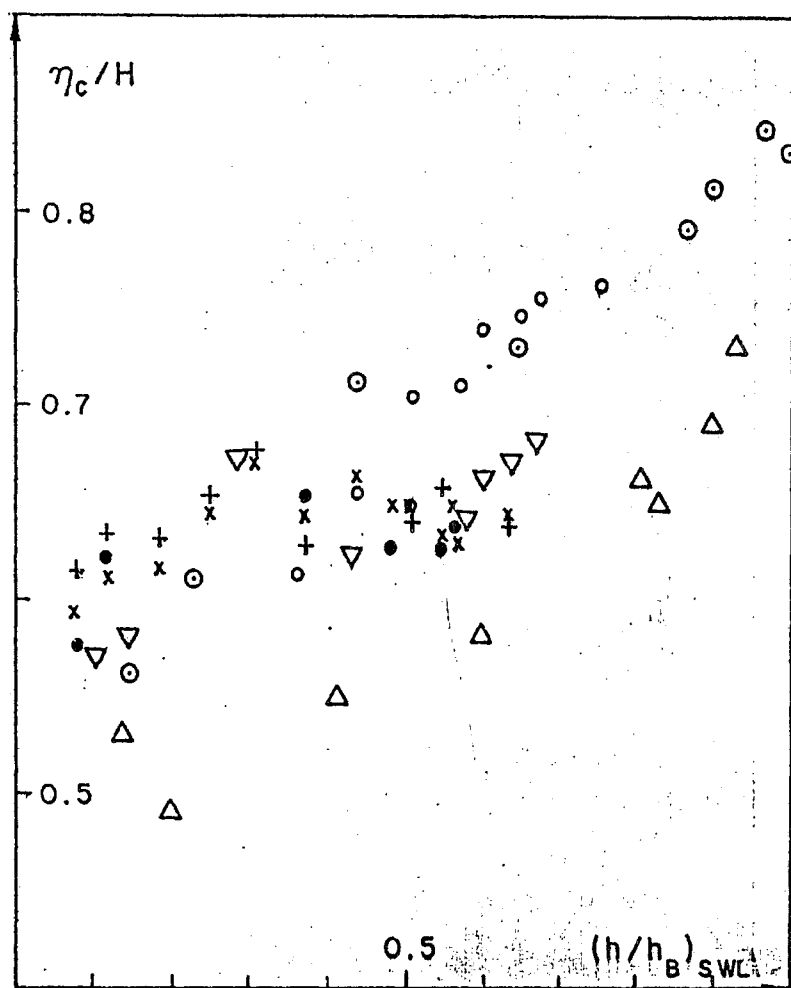
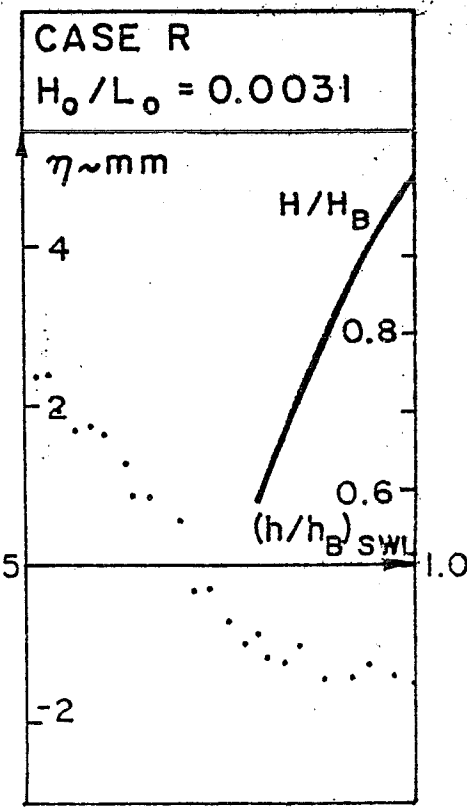
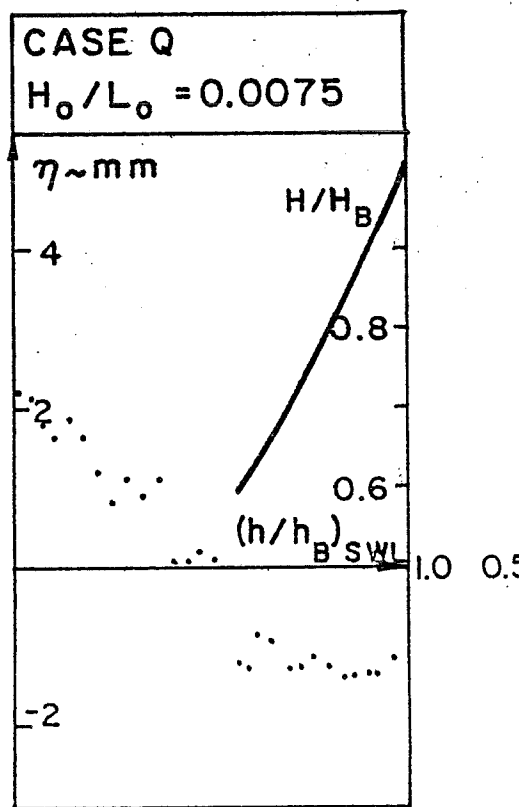
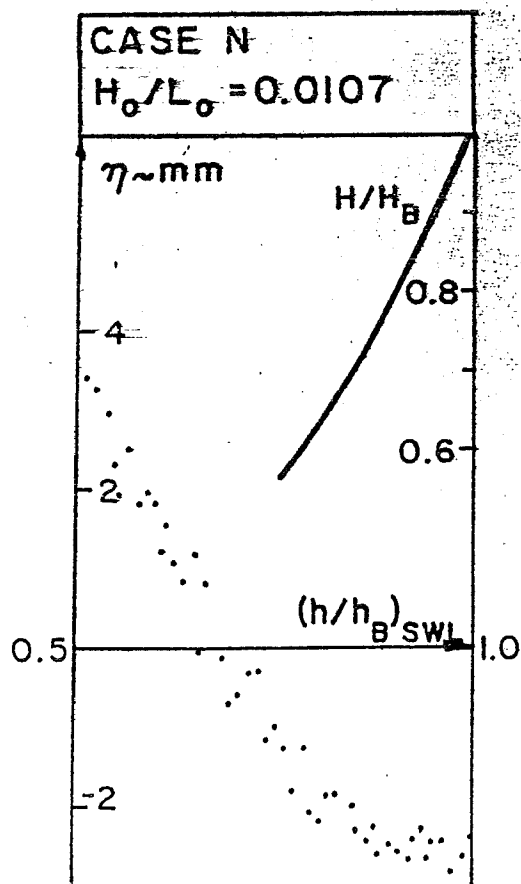
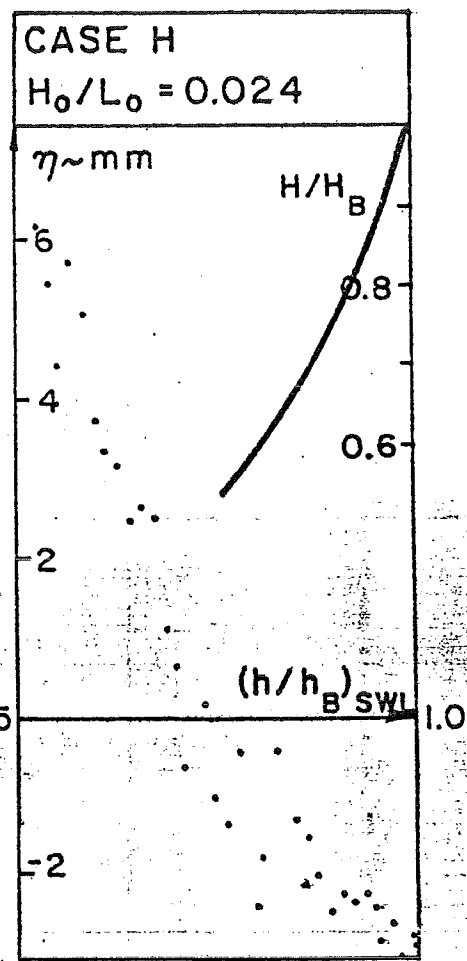
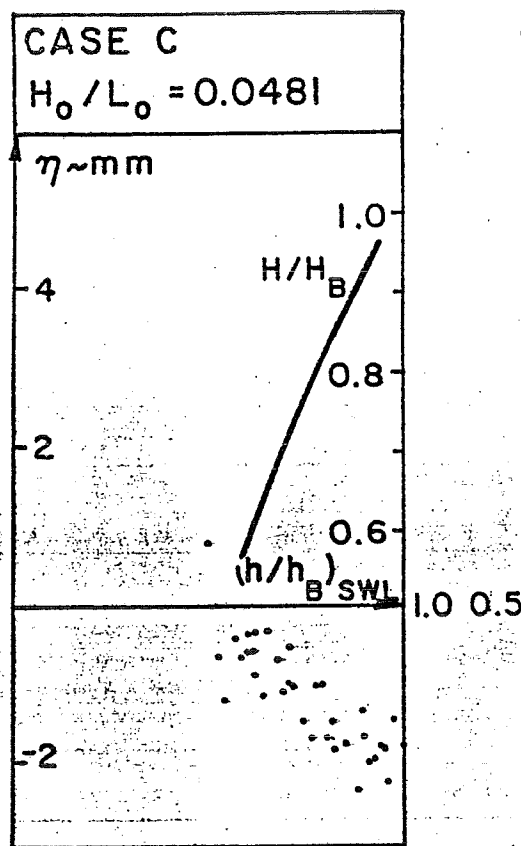
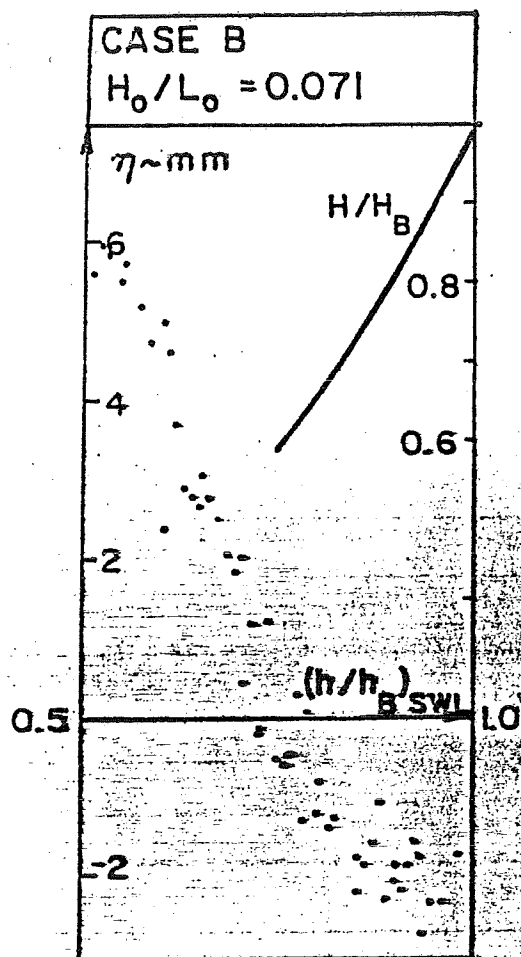


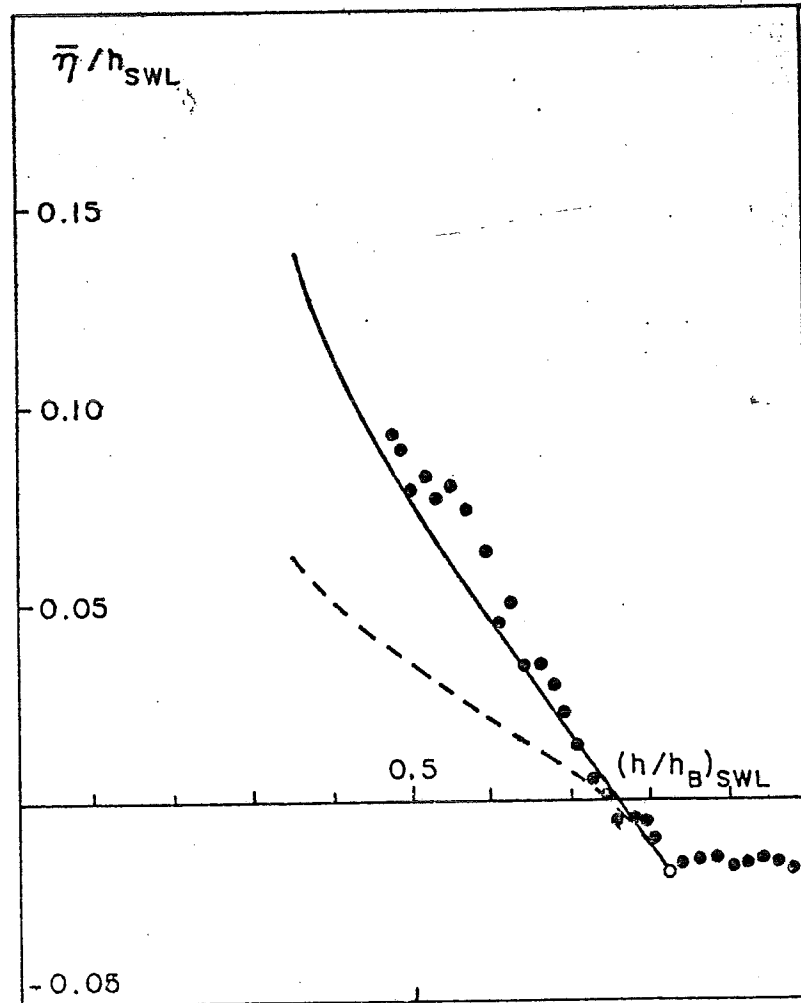
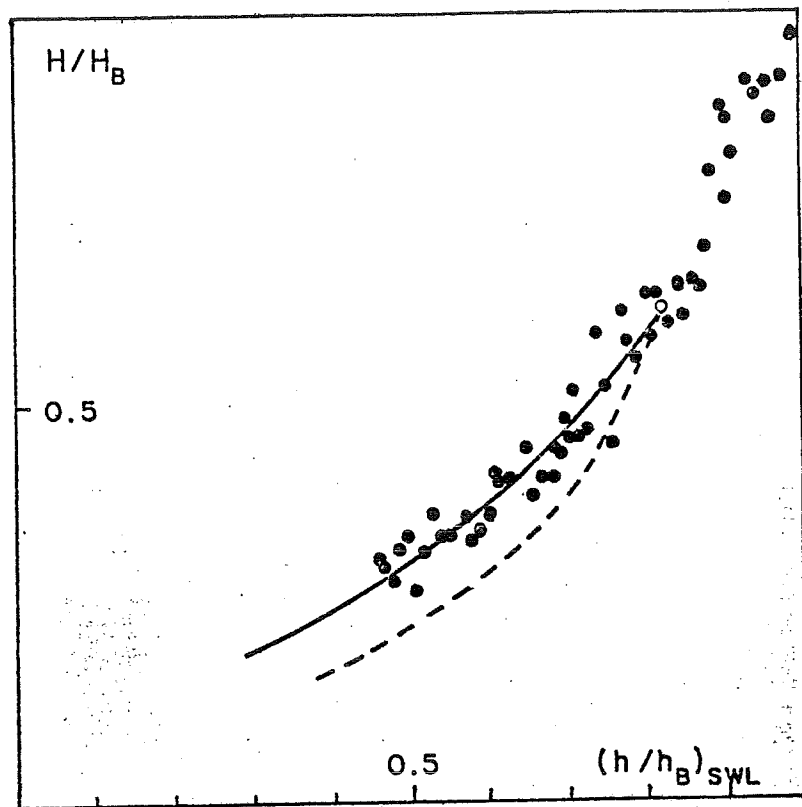
Fig 11



	H_0/L_0
•	0.034
+	0.034
x	0.034
○	0.0093
⊙	0.0053
△	0.0030
▽	0.0053

Fig 12





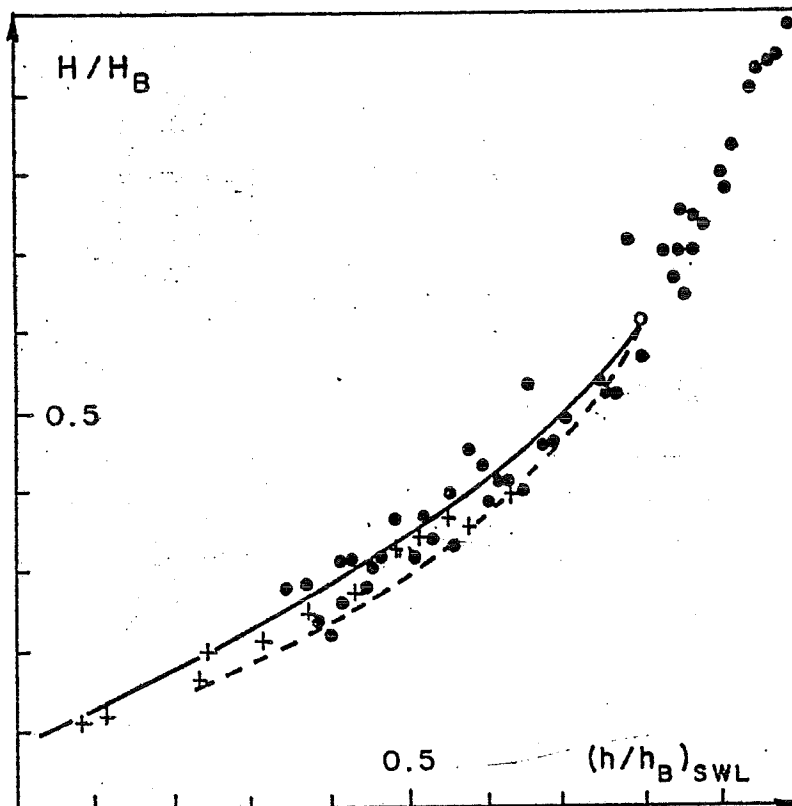


Fig 15 a

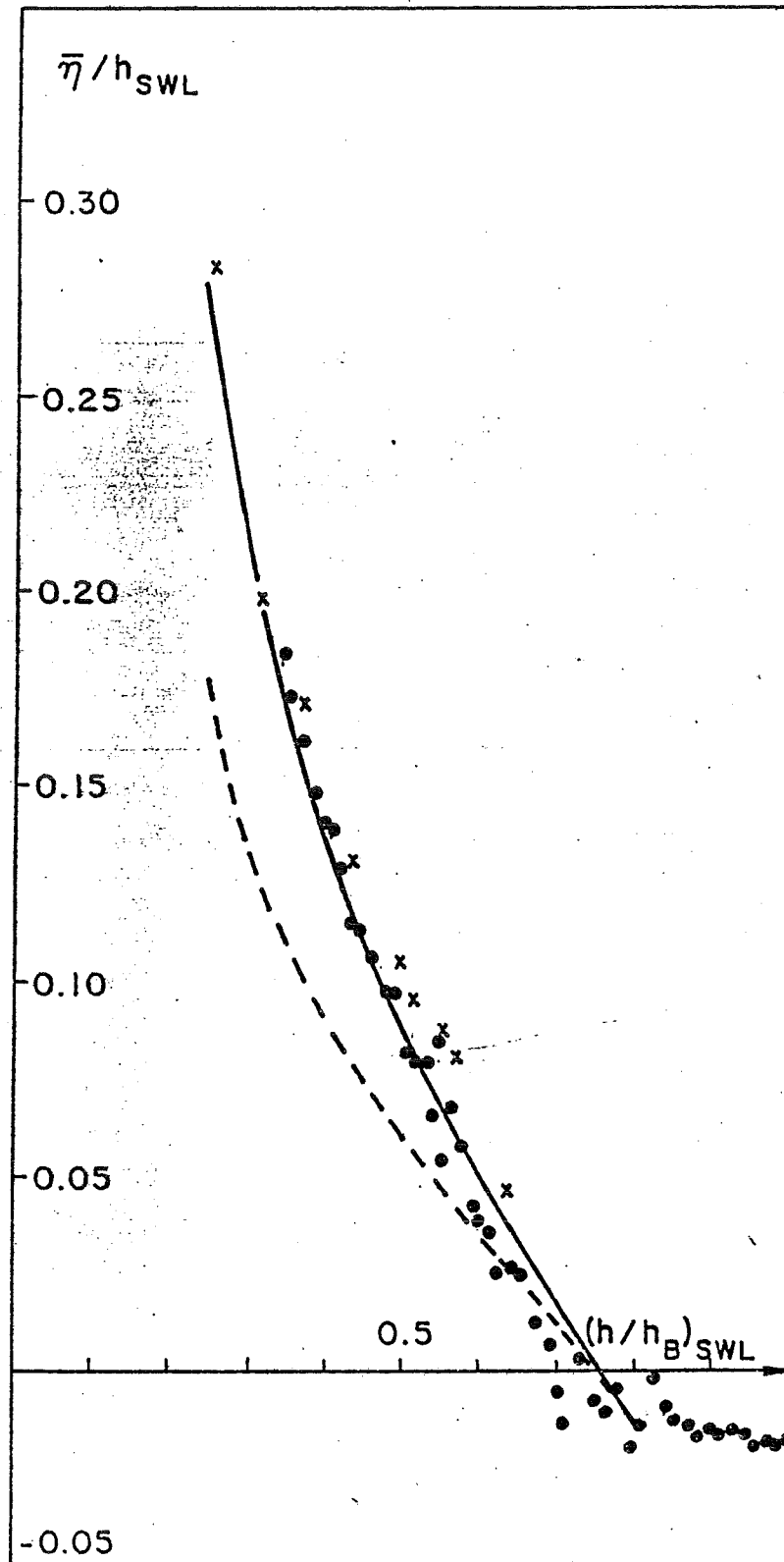


Fig 15 b

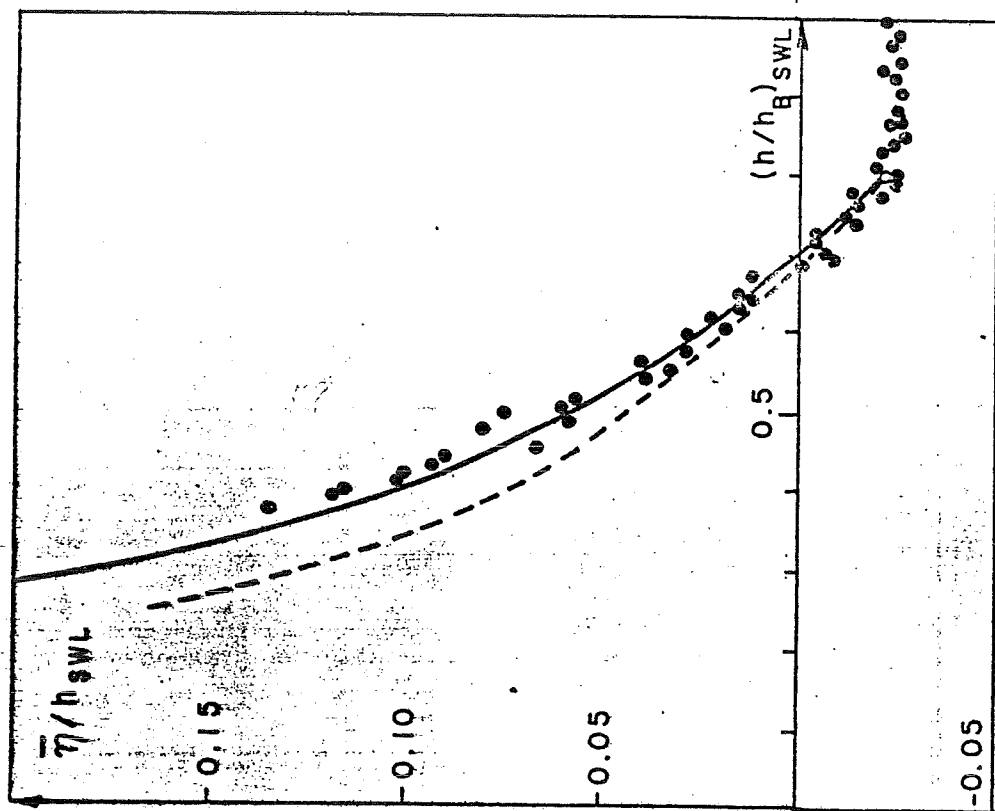
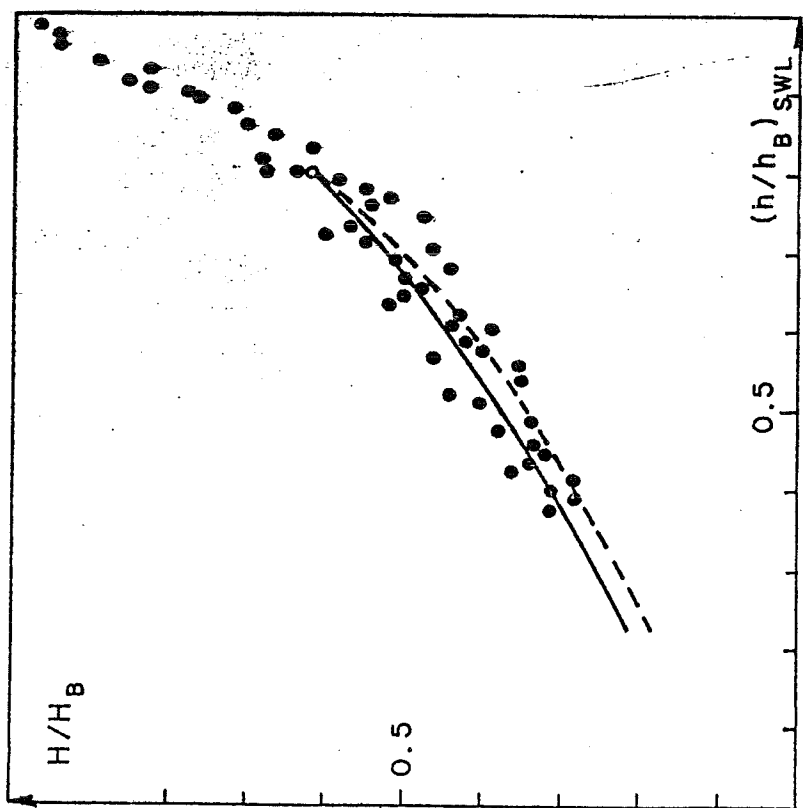


Fig 16

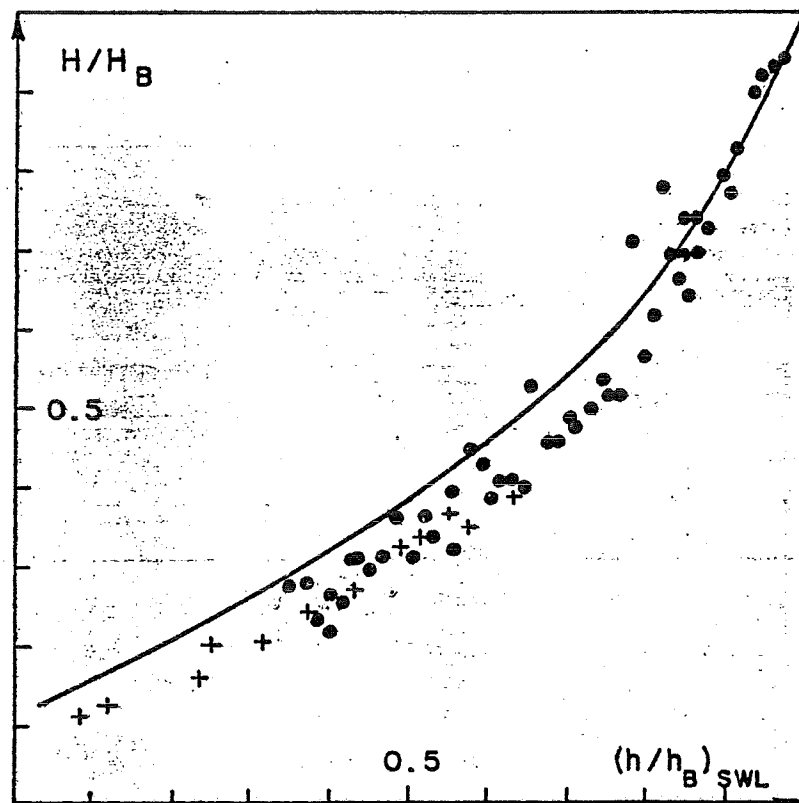


Fig 17

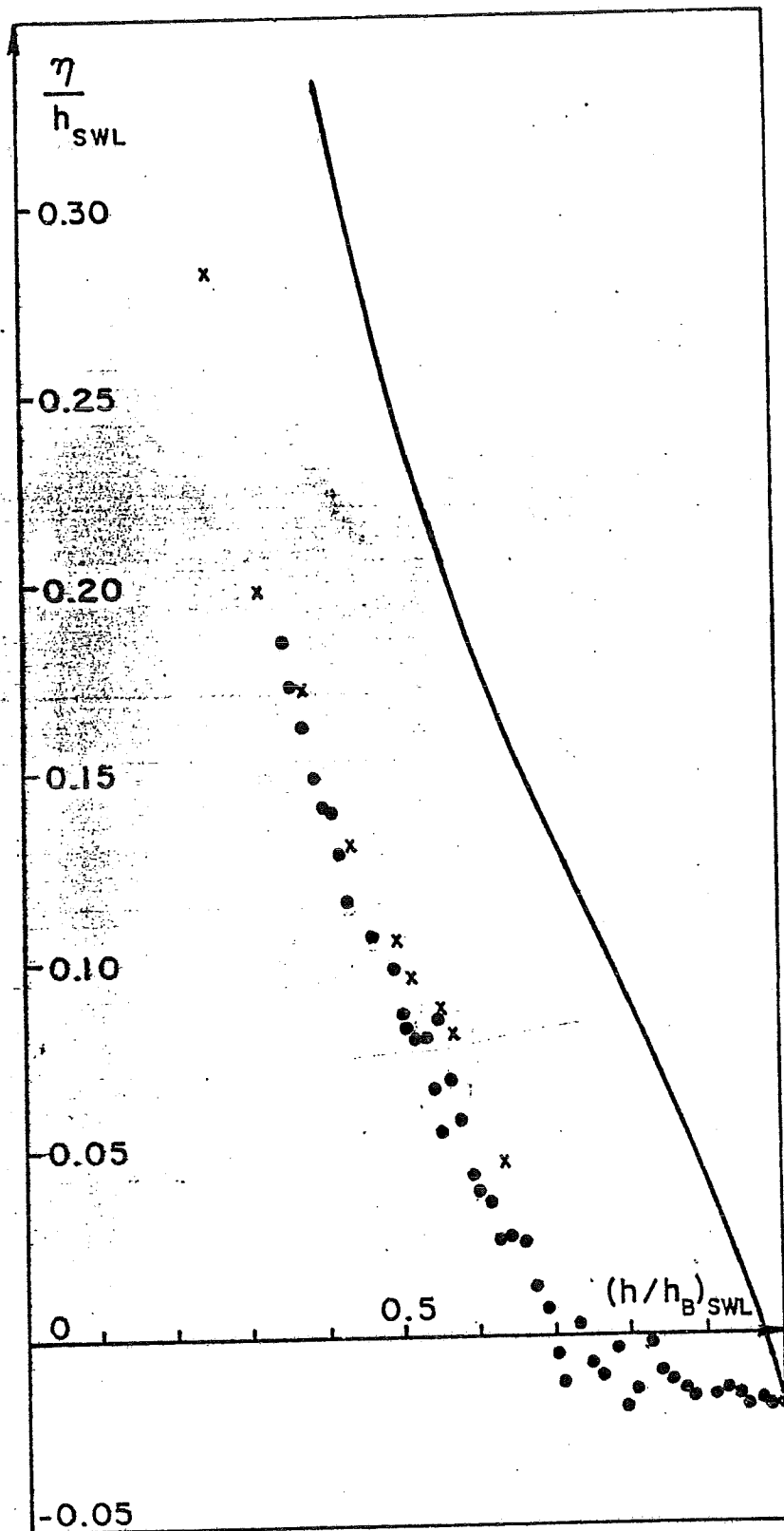


Fig 18

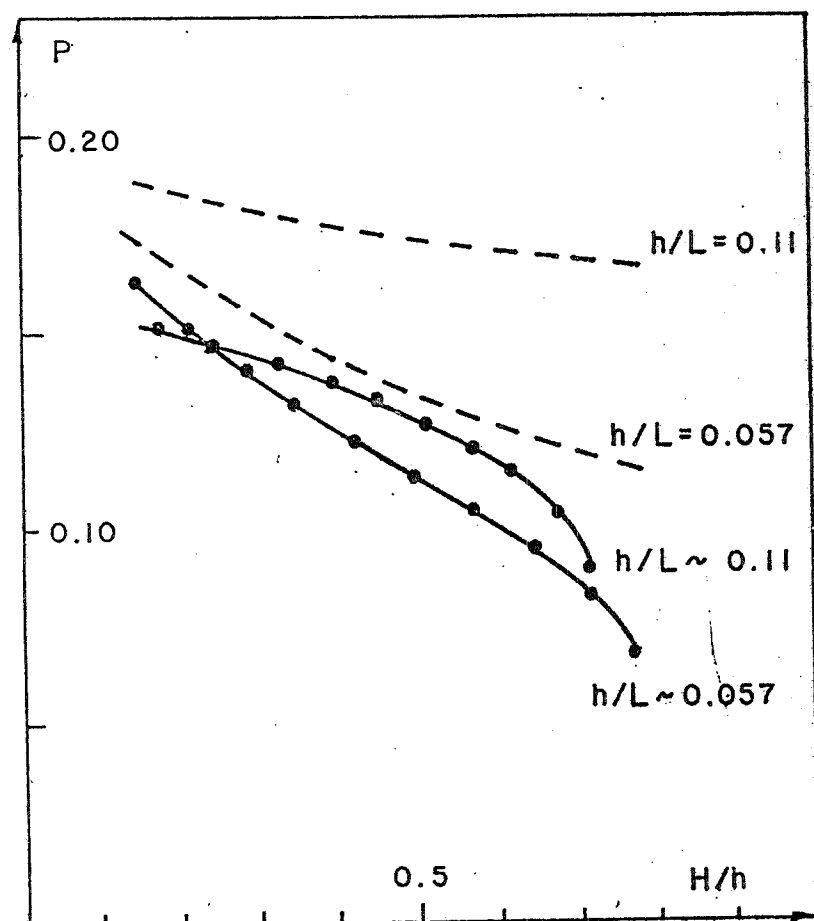


Fig 19

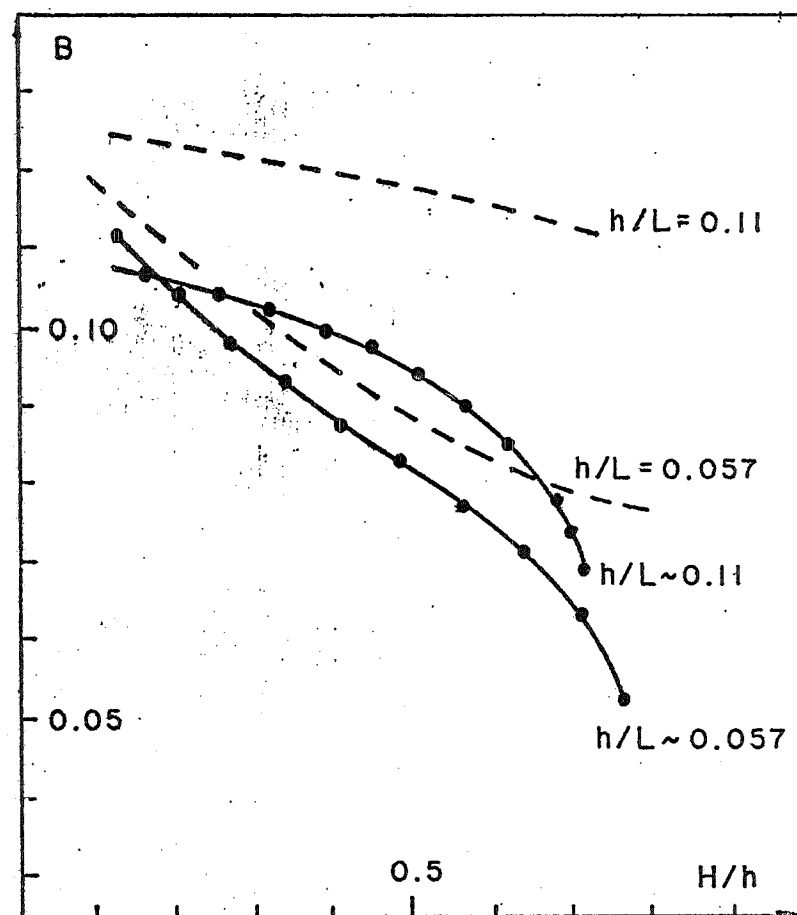


Fig 20

